2006

A rotational arm connection point design for a C-130 aircraft standardized sensor platform

Kenneth A. Williams
West Virginia University

A Rotational Arm Connection Point Design for a C-130 Aircraft Standardized Sensor Platform

Kenneth A. Williams

A thesis submitted to the College of Engineering and Mineral Resources at
West Virginia University
In partial fulfillment of the requirements for the degree of
Master of Science
in
Mechanical Engineering

James Smith, PhD., Chair
Kenneth Means, PhD.
Gregory Thompson, PhD.

Department: Mechanical and Aerospace Engineering
Major: Mechanical Engineering

West Virginia University
Morgantown, WV
2006

Keywords: Hub Design, Finite Element Analysis

ABSTRACT

Design of the Rotational Arm Connection Point for a Standardized Sensor Platform for a C-130 Aircraft

Kenneth A. Williams

West Virginia University's Center for Industrial Research Applications (CIRA) was sponsored by the United States Army National Guard (USANG) and the Department of Defense (DOD) to design a standardized, articulating sensor platform for the C-130 Hercules military aircraft. This sensor platform was to be capable of in-flight deployment and capable of facilitating a diverse spectrum of sensor configurations in order to aid in surveillance and reconnaissance for counter narco-terrorism efforts. Two complete sensor pallet prototypes have been developed. The current platform configuration consists of four aluminum arms that are connected to a rotational shaft via a cylindrical hub. For the construction of the third prototype of the sensor platform, an optimization of the rotational arm-hub connection was performed. The goal of the new design was to allow for easier system assembly, maintenance, and the ability to carry a larger sensor payload. The following work describes the complete design and development of the new arm-hub connection through the use of both analytical and finite element analysis (FEA) using Pro-Engineer and Pro-Mechanica solid modeling software.

Table of Contents **Page #**

Table of Contents **Page #**

Figures Listed **Page #**

Figures Listed **Page #**

Tables Listed **Page #**

Acknowledgments

There are several people to whom I owe thanks for helping me along the way in my engineering career. First and foremost I owe thanks to my parents, Dave and Tammie Williams, for all of their support and encouragement throughout all of my years in college. Without their support I would not have made it as far as I have today. Second I would like to thank the entire MAE faculty at West Virginia University for offering their guidance and taking time out of their busy schedules to assist in teaching me the fundamentals of engineering. I would like to extend a very special thanks to Dr. James Smith for allowing me to work under him in the pursuit of my graduate education and showing me what I am capable of accomplishing. If it was not for him I would have never extended my college education to the graduate level. I would also like to extend a thank you to my fellow students who have worked on this project with me, Zenovy Wowczuk, Seth Lucey, and Wes Hardin; they have been a lot of fun to work with and I have learned a lot from their knowledge and engineering skills.

CHAPTER 1: INTRODUCTION

1.1 System Background

Throughout its long history, the National Guard (NG) has had to fulfill a dual mission for the United States. That mission is to provide the nation with units trained, equipped and ready to defend the United States and its interests all over the globe and to protect life and property within the United States [1].

One of the biggest threats to life and property in the United States is the continuing presence of a large and often organized illicit drug trade, which supplies the United States with drugs sourced from home and abroad. The role of the National Guard in combating the drug trade is to support counterdrug law enforcement efforts by providing personnel and equipment resources. For the case of aircraft, these resources are limited to what is already in inventory with no immediate plans for large additions to the fleet [1].

The National Guard provides irreplaceable support to the Department of Defense as well as civilian sectors. Within this context, the National Guard, to meet its needs, leverages programs, research, and developed technology from a wide variety of sources. This includes government, university, industry, and non-profit organizations. With these and other groups, the National Guard focuses their efforts on the transferring and insertion of confirmed technologies and programs that will directly assist their missions. Similar to military and law enforcement agencies, the missions of the NG necessitate the investigation and implementation of field deployable and often time’s novel technologies to meet demanding and changing needs.

The National Guard has a requirement to support counterdrug law enforcement efforts through the National Guard Bureau counterdrug Office (NGB-CD). In this role, the NG provides resources, technical and personnel, to support civil authorities in counterdrug activities. To supplement this effort, the National Guard uses technology to enhance and advance counterdrug law enforcement agency efforts. The National Guard has only recently begun investigating using other aircraft (other than the C-26 and OH-58) in assistance with counterdrug missions. One of the most available and versatile aircraft in the National Guard fleet is the C-130 Hercules. The abundance of C-130 aircraft available to National Guard units across the United States and around the world gives it the immediate access advantage over other aircraft in the National Guard fleet [2].

The C-130 aircraft is manufactured by Lockheed Martin and has been produced since the mid 1950's. The primary mission of the C-130 is as a medium range tactical airlift and as the prime transport for paratroop and equipment drops into hostile areas. The C-130 has also been modified into specialized platforms including gun ships and electronic warfare platforms Figure 1 shows a C-130 aircraft in flight.

Figure 1 – C – 130 aircraft during flight

The C-130 aircraft encompasses a cargo floor approximately four feet above the ground, a roll on/roll off rear loading ramp, and an unhindered, fully pressurized cargo hold area. The C-130 is capable of holding more than 42,000 pounds of cargo distributed through four 463L pallet positions in addition to a rear cargo ramp pallet position. The 463L pallets are military standard pallets that are developed for use on the C-130 aircraft as well as other military aircraft. These pallets are easily maneuvered throughout the aircraft by a roller system integrated into the cargo hold and ramp. Another important feature of the C-130 aircraft is that it has the capability of flying while the rear cargo door is down. This feature was developed for the use of parachute drops during flight [1].

West Virginia University (WVU) was contracted to design a standardized roll-on, roll-off sensor pallet system for a C-130 aircraft. The idea was conceived by the National Guard and the Counter Narco Terrorism Technology Development Office to aid in the combat of drug trafficking in the United States. The system was constructed on a standard 463L type cargo hauling pallet, and consists of a sensor pod attached to four arms that suspends the pod from the rear cargo ramp of the aircraft. The system is initially stored completely within the body of the C-130 until deployment. During deployment the sensor pod and arms are rotated into position via an electric motor and a gear reduction box with two output shafts [3]. The model of the entire sensor pallet and its deployment are shown in Figures 2, 3, and 4.

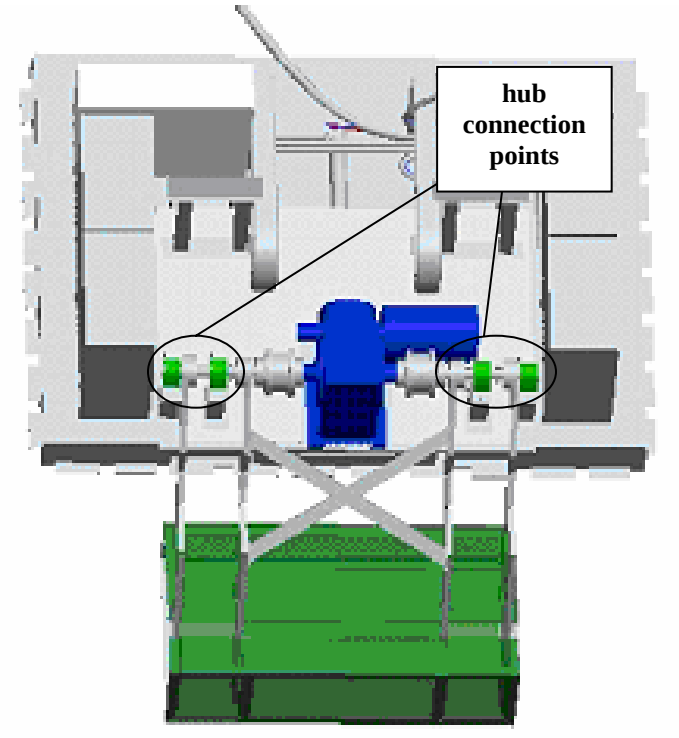

Figure 2 – Model of sensor pallet [3]

Figure 3 – Sensor pallet in stow position on a C-130 rear cargo ramp. [3]

Figure 4 – Sensor pallet in deployed position [3]

1.2 Current Hub – Arm Connection

The current hub – arm connection consists of four arms each 4 inches wide and 0.75 inches thick constructed of ASTM 6061 T-6 aluminum. The arms are attached to two (two arms per shaft) 2 inch solid steel shafts with 3/8 inch keyways via a circular steel hub through the use of six UNF 3/8- 24 grade 8 steel bolts arranged at a radius of 1.75 inches in a circular pattern around the hub at an angle of 60 degrees apart. The shafts are subjected to a static torque of 43,000 in-lb and when the dynamic loading conditions are taken into consideration, the shafts may experience moments up to 65,000 in-lb. The shafts are also subjected to a shear force of up to 1,000 pounds (depending on sensor configuration) due to the weight of the sensor pod, sensors, and arms. The current arm/hub shaft assembly is shown below in Figures 5 and 6.

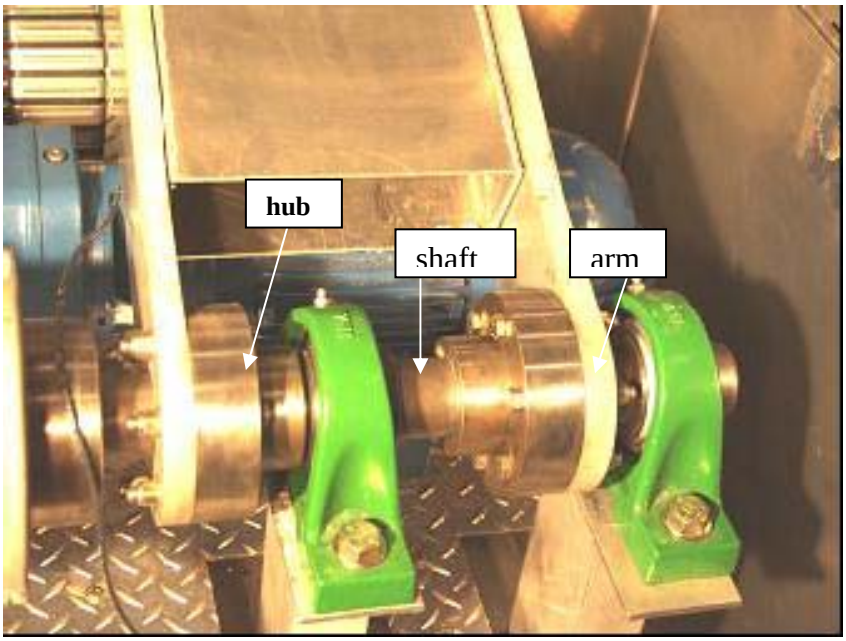

Figure 5 – Arm hub assembly and shaft attachment [3]

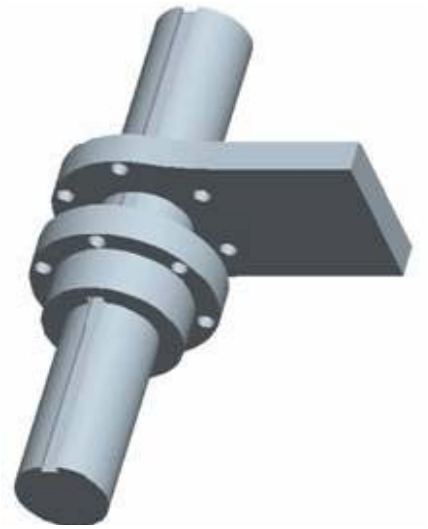

Figure 6 – Assembly Model of the rotational components [3]

1.3 Proposal for a New Hub – Arm Connection

The current hub – arm configuration introduces several complications into the pallet system during the assembly, maintenance, and operation of the rotational components. In order to correct these problems it was deemed necessary that the hub – arm connection point be redesigned.

The primary goal of this thesis was to develop a new arm – hub connection configuration for a standardized roll – on, roll – off sensor pallet system for a C – 130 military aircraft. The new hub design was specified to change the arm geometry in such a manor that the stress concentrations at the base of the arm due to the fillet are reduced or eliminated. In addition to reduction of the stress concentrations at the base of the arm, the new hub had to allow for easier assembly and removal of the rotational arms to the hubs for maintenance and manufacturing purposes, and to minimize the backlash in the hub – shaft connection point created by the shear keys in the current hub design. It is the purpose of this thesis to describe the complete design process which was carried out during the development of the new hub – arm connection assembly.

The new design consists of a steel hub connected to a solid 2 ½" steel shaft via a standard SAE class B 10 tooth spline. The rotational arms reside within a sleeve cantilevered from the rotational shaft which allows for the rotational arm to be placed completely outside of the shaft in order to enable direct removal of the arm without removal of the rotational shaft or bearings. The rotational arms are secured within the hub sleeve via four 9/16 inch bolts. The new shaft - hub configuration is shown below in Figure 7.

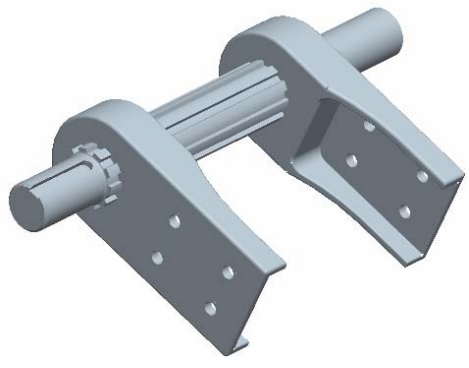

Figure 7 – New arm hub design

Chapter 2: LITERATURE REVIEW

2.1 History of Finite Element Analysis Method

Use of finite element methods for problem solving dates back to the year 1943 with the work of a mathematician named Courant [4]. Courant proposed breaking a continuum problem into triangular regions and replacing the fields with piecewise approximations within the triangles. The finite element method provides for a simpler way of solving large complex geometric problems, in which differential equations must be used, to an algebraic problem wherein the finite elements have the complex equations solved for their simple shape (triangle, rod, beam, etc.). A matrix of size equal to the number of unknowns for the element is then produced to represent the element which creates a linear algebraic relation and not a differential equation. The solution for the entire problem can then be solved by assembling the element matrices in the same manor as the real problem is built, with many simple pieces of material [5]. However in Courant's day this method of problem solving was impractical because of the complex algebraic equations created by assembling the element matrices. It was not until the late 1950's and early 1960's when computers came about, that it became feasible for the engineering community to integrate the finite element method into their design procedures. However at this stage the only people who could afford the technology were the large aircraft industries. In the early 1970's finite element software had been developed and by the 1980's microcomputers were developed capable of running finite element analyses. It was at this point in which the use of finite element analysis techniques became widespread among the engineering community. Today finite element

approaches are being used to solve engineering problems dealing with structures, heat transfer, magnetic fields, fluids, vibrations, and more.

2.2 Use of FEA for Initial Product Development

Traditionally in order to develop a product, engineers would have to create a prototype through the use of hand calculations which are based from assumptions of the component's behavior under design loading conditions. The prototype was then subjected to testing under the design conditions where flaws in the design would appear. Based on the nature of the design flaw the product would then be redesigned and tested again. This process would have to be repeated many times until a successful prototype was generated. With the introduction of FEA methods in the product development process, a more accurate portrayal of the component's behavior under loading conditions can be examined. The use of FEA software also allows engineers to spend less time solving for the component reactions to various loads and concentrate harder on the loading conditions and the development of a more accurate operation loading environment. This enables engineers to develop a prototype which will require a fewer number of design iterations and allow for the component to reach the production phase much faster and at a lower cost. Studies have shown that through the use of computer aided design a time savings of 27% and a cost savings of 32%, on average, have occurred in product development and production [6].

One example of the use of FEA methods in product development is exhibited by the Daimler Chrysler Corporation in which they performed a fatigue life analysis on their cast aluminum wheels. During the fatigue analysis they took into consideration the clamping force applied to the wheel disc as a result of the wheel's bolted connection to

the brake rotor. In order to perform the analysis, the wheel itself was modeled as well as the brake rotor, wheel bolts, tapered lug nuts, and shaft [7]. The wheel, bolts, nuts, and hub were meshed using hex dominant elements and the shaft was modeled using bar elements. A fine and high quality mesh was generated around the bolt holes and a matching mesh pattern was used in the contact pair between the tapered lug nuts and the nut seat on the wheel in order to prevent high stresses caused by the difference in mesh patterns and allow for easier initial convergence [7]. A static loading analysis was initially performed to determine the maximum stress values. The results of the static analysis were then implemented in the fatigue life analysis. For the fatigue life analysis a constant reversed loading condition was used for the stress-life analysis. The FEA software allowed the engineers to subject the clamped wheel to the rotary fatigue test conditions, as specified in the SAE test procedures, within a virtual environment. Because of this capability it was possible to test and alter the wheel configuration several times before a single piece of material was purchased. Once the design successfully passed the computer simulated design conditions, a successful testing of the prototype was achieved [7].

2.3 Use of FEA for Component Redesign

Many times in industry components of a particular machine will be replaced by different components and in some cases these new components impose loads on existing components which exceed the conditions for which the existing components were originally designed. One of the advantages of performing a finite element analysis on a component is the ease in which the loading conditions in the simulation can be varied, as well as the component material type and component geometry. This allows for an

efficient method of component redesign if problems are occurring with the operation of a machine. An example of the use of finite element methods for the redesign of a mechanical component was illustrated by Timoney Technologies Ltd. in their analysis and redesign of an independent suspension axle housing. The axle housing element performs multiple tasks such as housing the differential assembly, acting as an extremely stiff structural cross member of the chassis, and providing axle arms as anchor points for the suspension control arms [8]. The original design of the suspension system consisted of twin coil springs between the chassis and lower wishbone which met the fatigue performance criterion. When the suspension was redesigned to accommodate a single hydro-pneumatic strut the load paths through the suspension components were consequently altered and cracking of the axle housing began to occur. FEA was used to determine the new loading conditions experienced by the axle housing as a result of the change in suspension and to arrive at a solution which would allow the axle housing to withstand the specified number of 300,000 cycles to failure [8].

First an analysis was conducted on the existing axle housing subjected to the new loading conditions. The results of the analysis showed that the housing was failing after only 17,000 cycles at the junction between the central spine and the main body of the axle housing due to high tensile stress levels. They determined than a tensile stress of 380 MPa was the maximum stress for which the housing could be subjected to in order to achieve a life of 300,000 cycles. Through the use of FEA the shape of the central spine was altered in order to lower the stress in the region of concern to 274 MPa [8].

A second example of the use of FEA in component redesign is illustrated by Textron Automotive in their development of plastic interior trim components. A problem

was occurring with the door hooks which attach the door trim panels to the door sheet metal. When the panels were being assembled to the car sheet metal, the hooks were breaking. A study of the panel installation showed that as the panel was hung from the bottom hooks the operator would lean on the panel while connecting the wiring harness. Under this loading condition several hooks cracked and broke during pull testing. Through the use of an FEA analysis under the new loading requirements a finalized hook design which involved a longer hook and the use of a larger fillet between the hook and the substrate was implemented [9].

2.4 Use of FEA for Tooling Design

For production processes such as extrusion and forming, high pressures are used inside the die cavity and require some form of inserted tooling. Many of these inserts and dies themselves have complex, unsymmetrical geometry which are subjected to nonuniform loading. Without the use of FEA gross assumptions must be made in determining the behavior of the tooling under these loading conditions and an extensive trial and error process must occur to develop the tooling and inserts.

The Amcast Industrial Corporation is one company which employs the use of FEA in the design of their tooling for their FORMCAST^{TM} molding process. One piece of tooling for which Amcast used FEA to develop is that for the manufacture of an evaporator core inlet tube. This is a component of a car air conditioning unit which consists of a hollow tube with a flange at one end. The tube is formed from a hollow billet in which the blank is placed in a large upper cavity and a punch extrudes a portion of the metal into the smaller cavities to form a flanged tube [10]. Initially FEA was performed on a one piece tooling configuration which revealed that the stresses generated

at the flange corner of the die during the production process were very close to the yield stress of the material used for the tooling which predicts die failure at a low number of production cycles. Because of this an inserted tooling design needed to be employed in order to prevent premature die failure [10].

Initially a tungsten carbide insert was designed for the die because of its ability to withstand larger stresses; however, an FEA of this configuration still revealed large stresses in the remainder of the tooling [10]. In order to reduce these stresses FEA was performed on the insert being press fit into the die with various tolerances. Because no additional modeling of the components were required these analyses were easily carried out and it was determined that an interference of 0.123 mm provided for the lowest all around stresses on the system [10].

2.5 Use of FEA Throughout Product Development Cycle

Typically FEA is used in the early stages of product development. It is well known that FEA plays an important role in increasing the efficiency in which the initial design and development of a product is carried out. However this is only the initial stage of the product development cycle. After the product is designed it must travel through the manufacturing procedures. During this time several changes to the product may have to be made in order to facilitate a time efficient and cost effective manufacturability of the product. These changes may include changes in the material type or small changes in product geometry for such reasons as cost and ability to be produced on a large scale. If FEA is not implicated during these seemingly small changes to verify the functionality of the product, problems with the final product may occur.

Textron Automotive is one such company which employs the use of FEA throughout their entire production cycle. One example of this is their use of FEA throughout the development of plastic interior trim components. When the revised trim component described in section 2.3 was in the assembly phase, the door hooks were failing during the door slamming test [9]. A dynamic analysis was performed which showed that the stresses on the hooks were well within the allowable stress range for the material. Upon examination of the assembly it was discovered that the hooks were not being fully engaged in the sheet metal. Adjustments were made in the assembly procedure [9]. Upon proper instillation the hooks met the performance criteria [9]. Had the FEA analysis not been performed to verify the hook design, a redesign of the hooks would have most likely taken place. This would have cost a substantial amount of money because new tooling would have been required.

2.6 Summary

The cases cited in the previous sections have shown that the implementation of finite element analysis methods into the development of a product provide for a more accurate and efficient design process. It is for these reasons that finite element techniques were applied during the redesign process of the new arm – hub connection configuration. In addition to verification of the initial design of the arm – hubs, the solid model created during the design process can be easily tested under different loading configurations to test the structural integrity of the hub design if changes in the loading conditions occur.

CHAPTER 3: PROBLEM IDENTIFICATION

3.1 Increased Stress Concentration

The current hub configuration for the sensor deployment system consists of a circular disc to which the rotational arms are mounted. This circular hub has an overall diameter of six inches. Because of this, the base of the arms are required to have a circular geometry with a diameter of six inches in order to allow for the mating of the arms to the hub. Since the required arm height to support the loading of the sensor/pod configuration is only four inches, a fillet had to be incorporated into the arm geometry to step the arm height down from six inches at the hub connection to four inches for the remainder of the arm length. Due to this necessary arm geometry, high stress concentration areas resulted in the fillets around the circular hub. Pro-Mechanica was used to create a plot of the arm stresses during system loading. The analysis was performed by fixing the bolt holes at the base of the arm to simulate the arm being bolted to the rotational hub. Then a load of 375 pounds was applied to the end of the arm where the pod would be attached in order to simulate the resultant loads applied to the arms by the pod/sensor configuration. These high stress locations are illustrated in Figure 8.

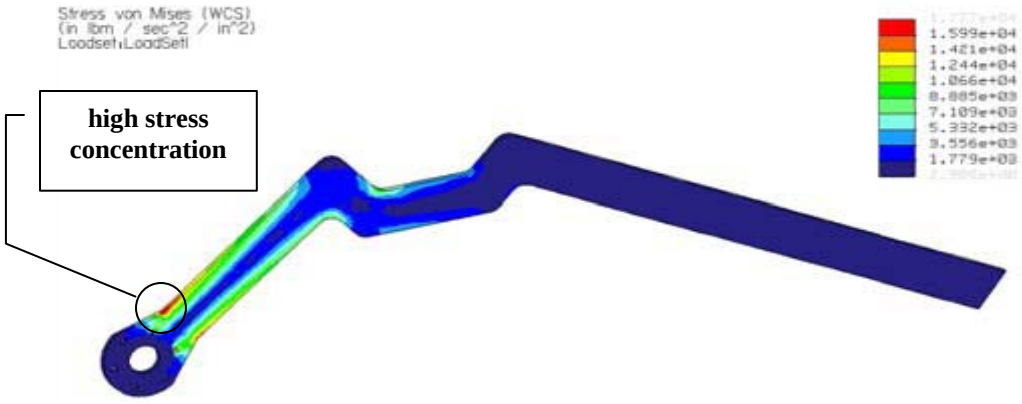

Figure 8 – Arm finite element analysis [11]

The primary goal of the new hub design is to change the arm geometry in such a manor that the stress concentrations in the fillet illustrated in Figure 8 are minimized.

3.2 Complex Assembly/Maintenance

With the development of any system which is anticipated to go into production, ease of assembly should be considered during the design procedure because a machine that can be easily assembled saves both time and money in the industrial world. With the current configuration of the arm – hub connection point the assembly process is longer than necessary. Since the arms must be slid onto the shaft in the same manor as the arm hubs, assembly of the rotational elements becomes complicated and cumbersome due to the shaft bearing configuration.

In addition to initial assembly of the rotational components, maintenance of the rotational arms is a complicated task. Since, during times of war, this system has the potential to be operating in a hazardous environment, damage occurring to the arms is very possible. If damage does occur to the system, it is desirable to have the system be repaired and operational as quickly as possible in order to continue flying missions. Also since the arms are constructed of aluminum and the hubs are steel, concerns for corrosion need to be addressed. In order to help prevent corrosion, the arms and hubs require the application of a corrosion inhibitor on the surfaces in which steel and aluminum are in contact. In order to ensure proper protection against corrosion the arms must be removed from the hubs during the application of the corrosion inhibiting agent. With the current arm – hub configuration, removal of one or more of the arms requires disassembly of the entire shaft, bearing, and hub components. This would provide for a system down time of at least several hours. The nature in which the arms must be assembled onto the hubs

requires an exceptionally long time which translates into a greater production cost. Also this complex assembly/disassembly makes maintaining the rotational arms a lengthy and labor intensive process which leads to increased system downtime during routine maintenance of the rotational components.

3.3 Problem Summary

In order to successfully redesign a component, the problems at hand with the original design must be clearly identified. Once the problems with the original design are identified clearly it is possible to address and correct those problems in the development of the new design.

With the current arm – hub design two problems are present. The first problem which must be addressed in the new hub design is that of the stress concentrations at the base of the rotational arms resulting from the fillet required to allow for the mating of the rotational arms to the hubs. Reduction of this high stress concentration in the arms will lead to a stronger and safer arm design. The second problem that must be addressed in the new hub design is that of the complex assembly and maintenance of the arm – hub connection. Developing a new hub design which will allow for easier system assembly and maintenance will provide a less expensive system assembly and a shorter system maintenance downtime.

CHAPTER 4: POSSIBLE HUB CONFIGURATIONS

4.1 Hub Geometries

In addition to reducing the stress concentrations in the fillet at the base of the rotational arm and allowing for easier assembly and maintenance of the rotational components, the new hub design was required to withstand the loads generated by a fully populated sensor pod which generates a moment of 65,000 inch-pounds, when combined with the weight of the sensor pod and rotational arms, on the rotational shaft – hub connection point. The new hub should also be designed in such a manor that failure due to fatigue would not be permitted. In order to meet these design requirements, several common arm – hub configurations were taken into consideration during the development of the new rotational hub design.

The primary and most important objective of the hub redesign was to reduce the stress concentration as a result of the fillet at the base of the rotational arm. The most obvious method of achieving this goal was to reduce the diameter of the existing hub from six inches down to four inches so that the arm height would not require a transition from four inches to six inches to accommodate the hub configuration. With no necessary transition area, the fillet which was creating the stress concentration area would not be required. An illustration of this idea is shown in Figure 9.

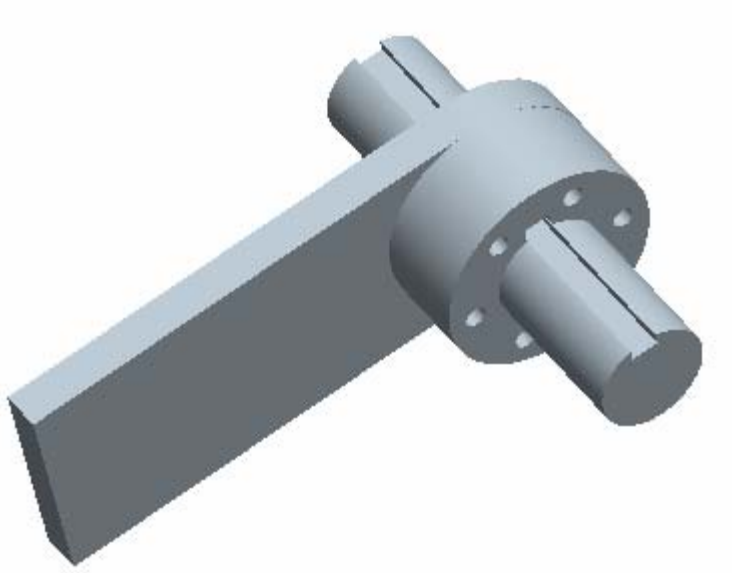

Figure 9 – Rotational arm – hub configuration with four inch hub

Although the arm – hub configuration illustrated in Figure 8 eliminates the fillet at the base of the arm, it does not allow for any easier assembly and maintenance of the arms. This is because the arm still encompasses the rotational shaft which requires that the rotational components be disassembled in order to remove and replace the arms. Because of this it was deemed that a circular hub configuration was not adequate to fulfill all of the design requirements.

Since a circular hub was not desirable, a second hub design was conceived. It was decided that the best method for eliminating the stress concentrations and allowing for ease of assembly and maintenance was to employ a circular hub with a cantilevered sleeve into which the arm end could be inserted. This would allow for the removal of the arm without the disassembly of the shaft, hub, and bearing components. The initial sleeve design consisted of a rectangular section into which the arm would be inserted and bolted in place, the sleeve would support the loads generated by the sensors and pod during

rotation and the bolts would prevent the arm from sliding out of the sleeve during deployment of the sensor pod. An illustration of this design is shown in Figure 10.

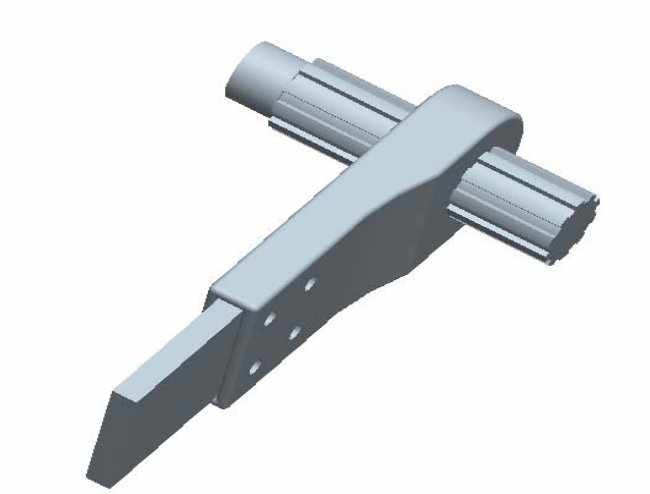

Figure 10 – Rectangular sleeve hub

While this hub configuration appears to provide a solution which meets the design requirements, a new set of complications would be imposed with the production and instillation of this hub design. The first problem encountered would be that of inserting the arms into the rectangular sleeve. In order to ensure proper performance of the hubs, the tolerance between the rectangular sleeve size and the arm cross section would have to be very small. Because the sleeve encompasses the entire arm, it would be extremely difficult to insert the arm into the hub by hand. Also corrosion of the aluminum arms within the steel hub would provide for extremely difficult removal of the arms from the hub sleeve in order to perform maintenance tasks. In addition to the difficulty of arm insertion and removal, the production of a hub with such a geometry would be extremely elaborate. Machining of the sleeved section of the hub would be nearly impossible because of its narrow width and length of depth. To manufacture such a hub would require the sleeved section to be heated and folded into shape and then welded into place.

In spite of the impracticality of this type of a hub production, the implementation of welds for the construction of the hub also presents another difficulty. Since the hub will be employed on an aircraft, an x-ray of all of the welded segments would be required to ensure a solid weld which contains no cracks or discontinuities. Also distortion of the material due to the high temperatures of the welding process may also cause problems with maintaining the required dimensional tolerances. Thus an alteration was required.

The final hub configuration considered was essentially the same hub pictured in figure 10. The only difference is that the rectangular cross section of the sleeve which holds the arm was changed to have a c-shaped cross section. This new design, which will be machined from solid steel, will meet all of the design strength and fatigue requirements and allows for the use of standard machining equipment for the manufacture of the hub. The c- channel geometry of the arm sleeve allows for easier assembly and disassembly of the rotational arms from the hubs and eliminates the stress inducing fillet at the base of the arm. The final hub design is shown in Figure 11.

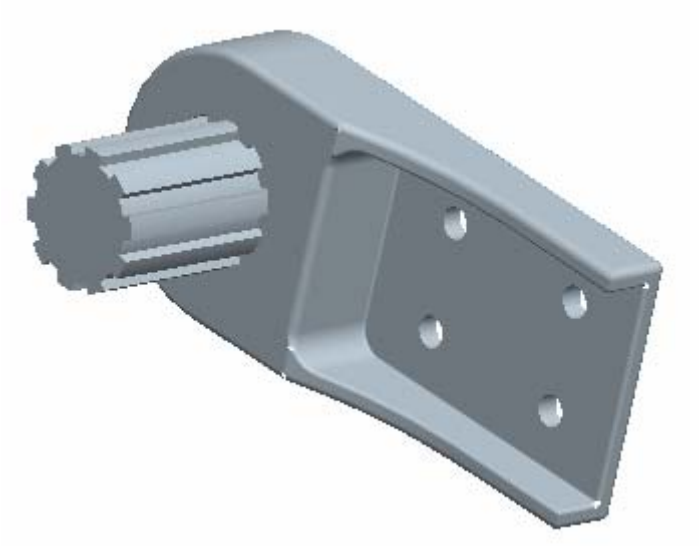

Figure 11 – Final hub configuration

4.2 Hub Connection Methods

With the use of a circular shaft for the rotation of an arm – hub configuration the hub must be secured to the shaft in a manner in which the torque applied to the shaft can be transmitted to the hub. Because the hub and shaft are both constructed from steel, welding the hubs to the shaft is one possible option for securing the hubs to the shaft. During the welding process local fusion of the parts to be joined occurs at there common interfaces. In order to construct a weld, heat is supplied by a controlled electric arc passing from an electrode to the material being welded. Typically, an inert gas or a flux is used to shield the weld zone from the atmosphere during the welding process, and a filler metal is introduced so that sound, uncontaminated welds result [12].

However a welded connection of the hubs to the shaft would introduce various problems. One such problem encountered through the use of welds is the creation of unfavorable residual stresses of high magnitude which may result from postcooling shrinkage. These residual stresses can result in unacceptable distortion of the weldment and can play a significant factor in the fatigue life of the welded component [12]. Fatigue stress concentration factors for various weld-zone critical points are listed in table 1.

Table 1 – Fatigue Stress Concentration Factors for Various Weld-Zone Critical Points [12]

Location	K_f
Heat Affected Zone of Reinforced Butt Weld	1.2
Toe of Transverse Fillet Weld	1.5
End of Parallel Fillet Weld	2.7
Toe of Tee-Butt Weld Joint	2

A second method for securing the hubs to the shaft, a method currently employed on the sensor pallet to secure the rotational shafts to the flex couplers, would be the

implementation of a shear key. A shear key configuration consists of a soft, ductile metal component (key), usually square, which resides in a channel cut into both the shaft and hub. The channels are constructed in such a way that half of the key lies within the shaft and other half lies within the hub. The length of the key varies depending on the specified loading conditions. The key should be constructed of a weaker material than the shaft and hub so and designed to carry the operational loads of the system only. Thus if a problem were to occur, such as a jamming of the rotating components, the key would shear in order to avoid damage to the more expensive machine components [12]. An illustration of a shear key assembly is shown in figure 12.

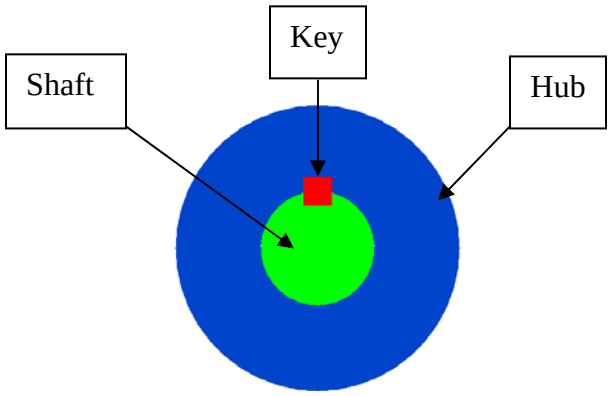

Figure 12 – Shear key assembly

The tolerances between the key and keyway are typically very close. For example for a 2 inch shaft, a ½ inch key is standard and the tolerance for the keyway width is +0.0000 to +0.0025 inches [13]. However some backlash does occur between the key and keyway during operation, especially if fluctuating torques occur. In order to prevent this backlash, it is common practice to include a setscrew in the design of the hub which will bear directly on the key. In some applications a second set screw may also be

included at 90 degrees from the key setscrew where it bears directly on the shaft [12]. Recommended key and setscrew sizes for various shaft diameters are shown in table 2.

Table 2 – Recommendations for selection of standard square parallel keys (abridged from ANSI standard B17.1-1967) [12]

Shaft Diameter Range (in)	Nominal Key Size (in)	Nominal Setscrew Size (in)
5/16 - 7/16	3/32	#10-32
1/2 - 9/16	1/8	1/4 - 20
5/8 - 7/8	3/16	5/16 - 18
15/16 - 1 1/4	1/4	3/8 - 16
1 5/16 - 1 3/8	5/16	7/16 - 14
1 7/8 - 1 3/4	3/8	1/2 - 13
1 13/16 - 2 1/4	1/2	9/16 - 12
2 5/16 - 2 3/4	5/8	5/8 - 11
2 13/16 - 3 1/4	3/4	3/4 - 10
3 5/16 - 3 3/4	7/8	7/8 - 9
3 13/16 - 4 1/2	1	1 - 8
4 9/16 - 5 1/2	1 1/4	1 1/8 - 7
5 9/16 - 6 1/2	1 1/2	1 1/4 - 6

When installed properly, shear keys provide an inexpensive and effective method of securing a hub to a shaft. However in certain situations shear keys can cause problems in machine design. In situations where large amounts of torque need to be transmitted, the length of key required to withstand the loading can become quite long. In certain situations, i.e. with shorter shafts, there is not enough room to accommodate a long shear key. Also a long key requires a hub with a thickness equal to the required key length which often times leads to an excessively large hub. Also human error in the installation of the hub onto the shaft along with the shear key is common. If the tolerances between the shear key and keyway are tight it is difficult to assemble the hub and key onto the shaft. In an attempt to make the assembly easier, the person installing the components often removes material from the key in order to allow it to slide into the keyway more

easily. By removal of material from the key, the tolerance between the key and keyway is increased and excessive backlash between the key and keyway occur during rotation, even when setscrews are used. A second downfall to a keyed connection is the stress concentrations created in the shaft/hub due to keyway geometry.

In such cases where high torques must be transmitted and shear keys become excessively long, an alternate hub connection is a splined connection. Splines are integral keys uniformly spaced around the outside of shafts or inside of hubs, as illustrated in Figure 13 [12].

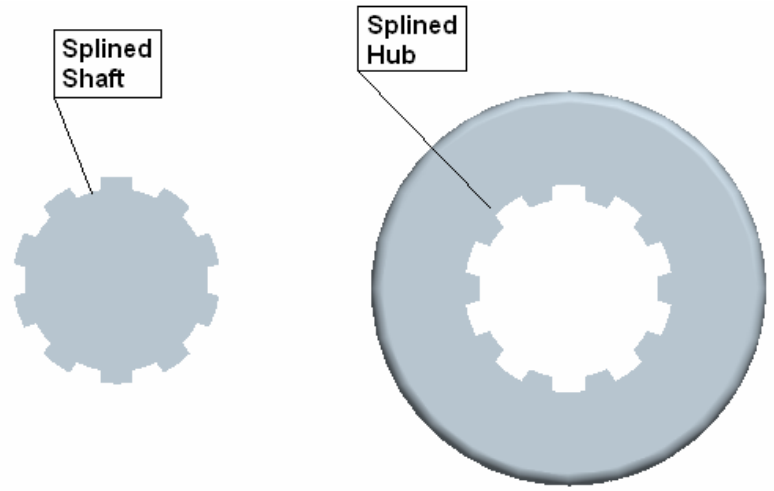

Figure 13 – Spline Geometry

For straight wall splined connections three classes of fit are obtainable. The first class is a class A fit which provides for a permanent connection that is not able to be moved after installation. The second class is a class B fit which will accommodate axial slide when no torque is applied to the splines, however while a torque is applied the splines will remain locked in place. The third class is a class C fit which will accommodate axial sliding while torque is applied to the splines [12]. One downside to splined connections is the cost to produce the splined segments. To produce the splines

requires spline size and type specific tooling and the time to machine the splines is substantially longer than that of a single keyway. A second downfall of a splined connection, which needs to be taken into consideration during the development of the splined connection, is the stress concentrations which occur at the base of the spline teeth.

4.3 Chosen Hub/Connection Configuration

After weighing the pros and cons of the different hub geometries it was decided that the circular hub with a cantilevered sleeve with a c – shaped cross section was the best choice for the new hub design. This hub eliminates the fillets at the base of the arm which cause high stress concentrations and at the same time allows for faster and easier assembly, maintenance and replacement of the rotational arms.

Due to the large torque to which the shaft and hubs are subjected, a splined hub connection was deemed the optimal connection configuration. Because the length of the rotational shaft is limited to the distance between the sensor boxes mounted to the sides of the sensor pallet, a splined connection was chosen in order to minimize the amount of shaft space occupied by the hubs. A splined connection also reduces the odds of improper installation caused by human error during assembly of the rotational components. A class B spline fit was chosen because it will not slide along the shaft during operation of the sensor platform but will still slide easily onto the shaft once the loading on the splines is removed.

CHAPTER 5: DESIGN LOADING CONDITIONS

With the design of any mechanical component, an understanding of the loading conditions to which the component will be subjected is essential in order to conduct a thorough design. The primary functions of the rotational arm – hubs are to transmit the torque from the output shafts of the gear reducer to the rotational arms and to secure the arms to the rotational system. In order to meet these requirements the hubs must be able to handle at least as much torque as the gear reducer is capable of producing and the connection point of the arms to the hubs must be strong enough to withstand the loading produced by the rotational arms and any components attached to the arms.

The gear reduction system is a Textron model CDBM0057716-A9 gear reducer which transmits 65,000 inch pounds of torque to the rotational shafts [14]. Thus, the design torque for which the hub – shaft connection must be capable of transmitting is 65,000 inch pounds.

Now that the design load for the hub – shaft connection has been determined, the loads imposed on the hub – arm connection must be determined. The objective for the sensor pallet system is to be capable of flying a variety of sensor configurations. Because of this need, the loads at the arm connection point are variable and a maximum sensor pod, arm, and sensor weight had to be developed in order to define the design loading conditions. It was estimated that the weight of the sensor pod, rotational arms and sensors act at 43 inches from the shafts axis of rotation. It was determined that a total sensor, pod, and arm weight of 1,500 pounds acting at a distance of 43 inches from the axis of rotation, which produced a moment of 65,000 inch – pounds, was the maximum capacity

which would still allow for rotation of the system. However to implement only a static analysis in the design of the arm – hub configuration would be inaccurate.

Since the arms rotate from rest to their deployed position and stop, then rotate to their retracted position and stop, acceleration must occur in order to bring the arms from rest to their rotational speed. During rotation, two forms of acceleration occur. The first form of acceleration is radial acceleration which acts along a line that runs from the center of the rotating mass along the radius of rotation and is determined by the radius of rotation and the tangential velocity of the rotating mass. The second form of acceleration is tangential acceleration which acts along a line that runs through the center of the rotating mass and tangent to the circle rotation, perpendicular to the radius, and is determined by the radius of rotation and the angular acceleration of the rotating mass. Newton's second law (F = ma) shows that these accelerations apply additional dynamic forces on the rotational system [15]. The action of these additional rotational forces is shown in Figure 14.

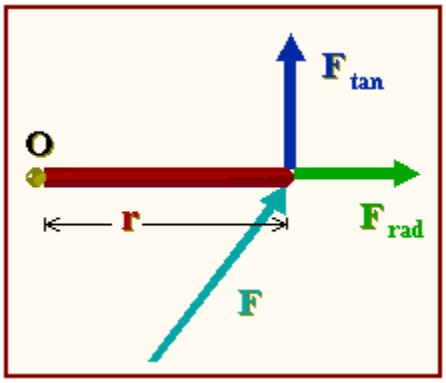

Figure 14 – Illustration of dynamic rotational forces [16]

The effect of these dynamic forces must be taken into consideration in order to produce an accurate design. It was decided to implement a dynamic load factor of 1.5, as required by the Federal Acquisition Regulation (FAR) [19], into the design to

compensate for the additional dynamic forces. With the addition of this dynamic load factor into the development of the maximum sensor pod, arm, and sensor weight, the original combined weight of 1,500 pounds had to be adjusted to only 1,000 pounds. It was estimated that the combined weight of the sensor pod and rotational arms is 200 pounds which allows for a sensor payload of 800 pounds.

In summary the design loads for the rotational system were viewed as a 1,500 pound mass acting at a point 43 inches from the rotational shafts axis of rotation. This induces a torque of 65,000 inch pounds on the arm – shaft connection region as well as a 1,500 pound normal shear force in that region. The loading model is shown in Figure 15.

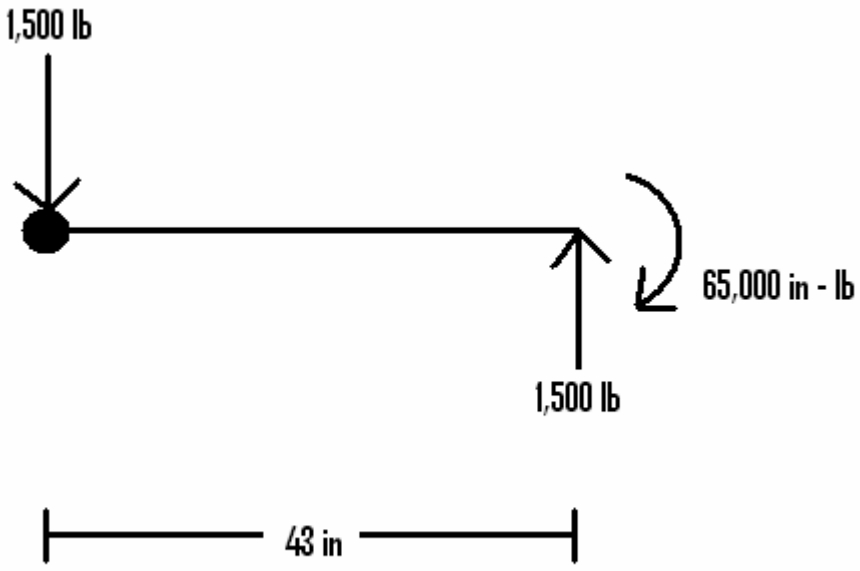

Figure 15 – Design loading model

CHAPTER 6: ROTATIONAL SHAFT DESIGN

In addition to determining the root diameter of the shaft required to carry the loading created by the sensor pod, arms, and sensors, design of the rotational shaft includes two separate connection configurations. First the rotational shaft must first be coupled to the output shaft of the gear reducer. This is accomplished through the use of a Faulk 100 series flex coupler. This series of flex coupler incorporates the use of a shear key to transmit the torque from the gear reducer to the rotational shaft. The second connection configuration is that of the rotational arm – hubs to the rotational shafts. The desired connection configuration to transmit the torque from the rotational shafts to the rotational arms is that of a standard SAE straight wall spline with a class B fit.

6.1 Shaft Root Diameter Design

The rotational shaft incorporated on the previous sensor pallet systems was constructed of 2 inch solid steel. The use of a rotational shaft of the same diameter as those implemented on the previous pallet systems was desired because it would allow for the use of most of the same shaft installation components incorporated on the previous sensor pallets (i.e. flex couplers and rotational bearings) to be incorporated on the new pallet system and would allow for the previous pallet systems to be retrofitted with the new arm – hub system at a minimal cost. In order to achieve this, an analysis was performed for a 2 inch solid steel shaft constructed of AISI 4130 steel under the specified loading conditions. The analysis was carried out as follows.

The primary load of concern for the rotational shaft was the torsion due to the combined weight of the sensor pod, arms, and sensors along with the inertial forces due to rotation of these components. The total torque placed on both shafts when adjusted

with the dynamic load factor of 1.5 is 65,000 inch pounds. Since there are two shafts the torque applied to each shaft was 32,500 inch pounds. The shear stress due to torsion was calculated using the following equation [17]:

$$\tau = \frac{Tc}{J} \ , \qquad (1)$$

where T equals the torque applied to the shaft, c equals the radius of the shaft, which equals 1 inch, and J equals the polar moment of inertia the polar moment of inertia of the shaft was calculated using the following equation [17]:

$$J = \frac{\pi d^4}{32}, \qquad (2)$$

where d equals the diameter of the shaft, which equals 2 inches. These equations gave a shear stress value of 20,690 psi in the shaft due to torsion. With a maximum allowable shear stress equal to 36,351 psi [18] a safety factor of 1.8 was obtained. The shaft is also exposed to a normal shear load due to the loading of the sensor pod and arms of 1,500 pounds which is dispersed evenly throughout the four arms to produce a shear force of 375 pounds which produces such a small shear stress that the effects of this loading were considered negligible. The results of these calculations verified that a solid steel shaft with a 2 inch root diameter, shown in Figure 16, is sufficient to support the torsional loading requirements.

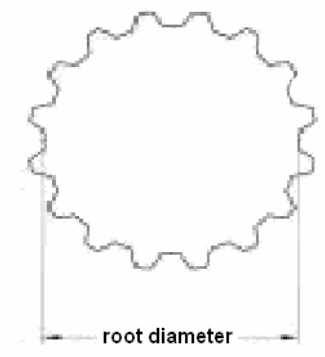

Figure 16 – Shaft root diameter

In addition to the hand calculations, Pro-Mechanica was also used to analyze the response of the shaft to the specified design loading conditions. In this analysis a 2 inch solid steel shaft was modeled. One end of the shaft was fixed while two point loads equal to 16,250 pounds were applied at the opposite end of the shaft to generate a moment of 32,500 inch pounds. The Model of the shaft with the applied loading conditions is shown in Figure 17.

Figure 17 – Static loads applied to shaft root diameter

The results of the finite element analysis of the shaft root diameter produced from the model shown in Figure 17 generated stresses around 40,000 psi within the shaft. Because the stresses produced in Pro-Mechanica were nearly twice as large as those calculated by hand. This was due to the manor in which Pro-Mechanica applies the loads to the model. In order to generate a moment in a shaft forces must be applied to one end of the shaft tangent to the shafts outer circumference. Pro-Mechanica allows for only two

nodes onto which the moment generating loads can be placed. Placing the forces on only two nodes generates high point stresses around the load application points. These high stresses will oftentimes skew the results of the analysis. Because of this shaft was modeled in ANSYS, which allows for the placement of the moment generating forces at several locations around the shaft circumference to alleviate the high point stresses and produce more accurate results. The shaft was then meshed using solid brick 8 node 45 elements. The ANSYS analysis produced stresses around 22,351 psi within the shaft. These values were within 10 percent of the hand calculations. The Von Mises stress plots for both the Pro-Mechanica and ANSYS analysis can be found in Appendix A.

6.2 Shear Key Design

The keyway for the Faulk 1090T flex coupler which is used to couple the rotational shaft to the gear reducer output shaft utilizes a standard shear key for a 2 inch shaft of ½ inch square [13]. The keyway cut into the flex coupler for the 2 inch shaft is 3 inches long. This limits the key engagement to only 3 inches. In order to ensure that 3 inches of key engagement was sufficient an analysis of the shear key was performed. For the key, potential critical sections include the shear plane between the shaft and hub and the contact planes between the sides of the key and the sides of the keyway. The analysis of the shear plane between the shaft and hub was performed using the following equation [12]:

$$\tau_s = \frac{2T}{Dwl} \quad , \qquad (3)$$

where T equals the torque applied to the shaft, which equals 32,500 inch – pounds, D equals the shaft diameter, w equals the width of the shear key, and l equals the length of key engagement. Evaluation of equation 3 at the design loading conditions and design

configuration showed that a shear stress of 21,667 psi would occur along the plane between the hub and shaft through the shear key. This provides for a safety factor of 1.7.

The analysis of the contact planes between the shear key and keyway was conducted using the following equation [12]:

$$\sigma_c = \frac{4T}{Dwl}, \qquad (4)$$

where T equals the torque applied to the shaft, which equals 32,500 inch – pounds, D equals the shaft diameter, w equals the width of the shear key, and l equals the length of key engagement. Evaluation of equation 4 at the design loading conditions and design configuration showed that a bearing stress of 43,334 psi would occur between the shear key and keyway. This provides for a safety factor of 1.45.

In addition to the hand calculations, Pro-Mechanica was also used to analyze the response of the shear key and keyway to the specified design loading conditions.

First an analysis of the shaft keyway was performed. In order to conduct this analysis, the shaft was modeled with a 3 inch keyway cut into one end, the outer surfaces of the shaft were fixed and a load of 32,500 pounds was applied to one wall of the keyway to simulate the effects of the key pressing against the keyway wall under the design loading conditions. The Model of the shaft keyway with the applied loading conditions is shown in Figure 18.

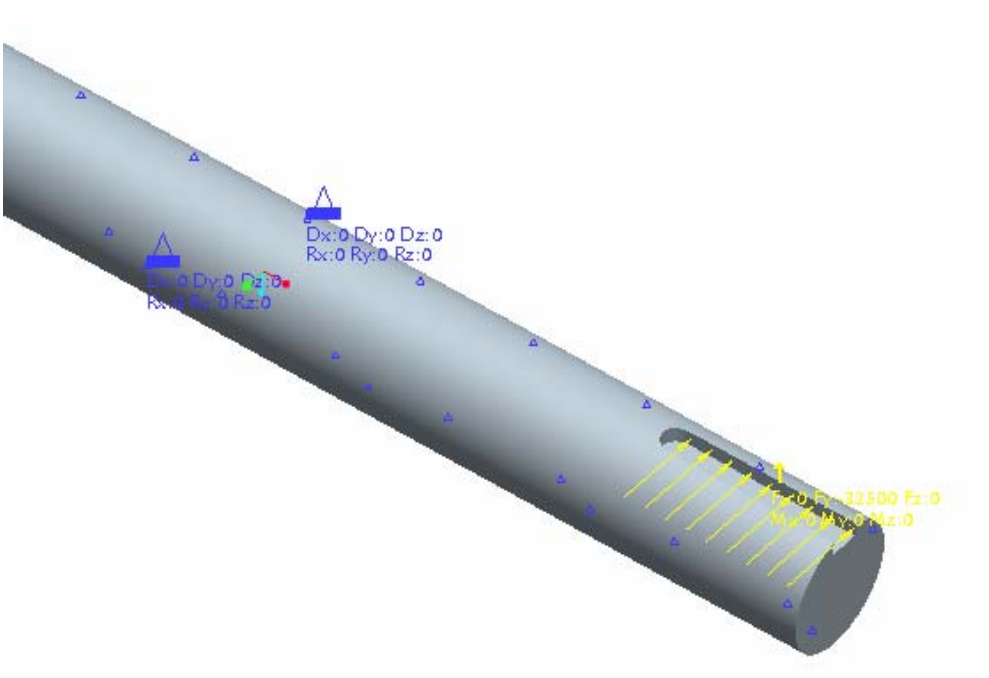

Figure 18 – Static loads applied to shaft keyway

The results of the finite element analysis of the shaft keyway produced from the model shown in Figure 18 generated stresses around 45,000 psi within the keyway.

Second an analysis of the shear key was performed. In order to conduct this analysis, a ½ inch square key 3 inches in length was modeled, three sides of the key were fixed and a load of 32,500 pounds was applied to the lower half of one side of the key to simulate the effects of the key pressing against the keyway wall under the design loading conditions. The model of the shear key with the applied loading conditions is shown in Figure 19.

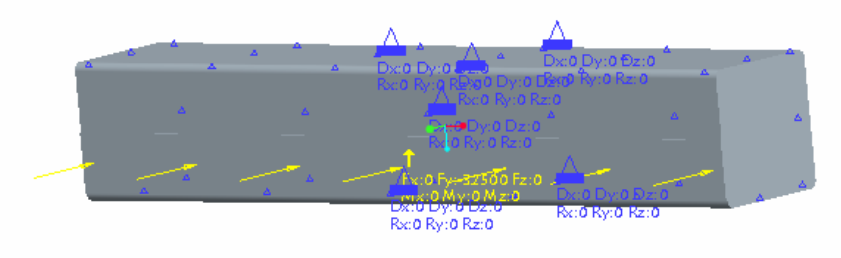

Figure 19 – Static loads applied to shear key

The results of the finite element analysis of the key produced from the model shown in Figure 19 generated stresses around 45,000 psi within the key.

The values for both the shear key and shaft keyway were within 10 percent of the hand calculations. The Von Mises stress plot for the Pro-Mechanica analysis of both the shear key and shaft keyway can be found in Appendix A.

6.3 Spline Design

In order to finalize the design of the rotational shaft, the splined portion of the shaft had to be determined. It was determined that a 2 inch root diameter of the rotational shaft was required to support the loading of the sensor pod, arms and sensors. Thus the overall diameter of the shaft into which the splines would be cut has to be larger than 2 inches. In order to minimize the cost of the shaft, it was desired to have the overall shaft diameter as small as possible. The root diameter of a given spline configuration is determined by two factors. The first factor is the overall shaft diameter and the second factor is the spline type. The spline type chosen for this application was a standard SAE 10 tooth straight spline with a class B fit. The relationship between the root diameter and overall diameter for this type of spline is shown in equation 5 [12]:

$$d = 0.860D \text{ , } \qquad (5)$$

where d equals the shaft root diameter and D equals the shaft overall diameter. Based on this equation it was determined that the closest standard shaft size which would still allow for a 2 inch root diameter would be a 2 ½ inch overall diameter shaft.

The final shaft design consisted of a 2 inch root diameter shaft with a ½ inch keyway 3 inches in length cut into one end and a 2 ½ inch diameter midsection into

which a standard class B SAE 10 tooth straight spline is cut. The model of the final shaft design is shown in Figure 20.

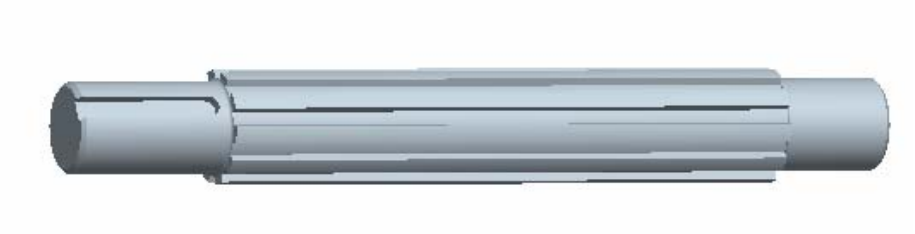

Figure 20 – Final shaft design

CHAPTER 7: HUB DESIGN

7.1 Length of Spline Engagement

Once the shaft diameter and spline configuration were determined, the design of the hub was begun. The first consideration was the length of spline engagement required to support the design loading conditions. The design loading conditions consisted of a combined pod and arm weight of 1,000 pounds acting at a center of gravity of 43 inches from the shaft center of rotation. This resulted in a static torque of 43,000 inch-pounds applied to the shaft. In addition to the static loading there is also a dynamic loading of the rotational system caused by the inertial forces of the pod/arms and sensor payload during rotation. Because of this a dynamic load factor of 1.5 was chosen to account for the additional rotational forces. The total design torque applied to the shaft with the dynamic load factor is equal to 65,000 inch-pounds. Since this load is to be carried equally by all four arms the design torque per hub is equal to 16,250 inch-pounds. Studies have shown that about 25 percent of the teeth carry the load in a splined connection [12], thus the length of spline engagement required to support the design torque was calculated using the following equation [12]:

$$l_{sp} = \frac{2T}{0.25d\left(\frac{\pi d}{2}\right)\tau_d}, \qquad (6)$$

where

T = torque applied to the hub,
d = shaft root diameter, and
τ_d = material shear yield stress.

$$\tau_d = 0.577 S_y, \qquad (7)$$

where S_y = material tensile yield stress.

Since AISI 4330 steel was chosen for the hub material the resulting length of spline engagement was calculated to be 0.30 inches. In order to meet proper safety requirements a length of spline engagement of 2 inches was chosen to give a design safety factor of 4.09.

In addition to the hand calculations, Pro-Mechanica was also used to analyze the response of the splined connection to the specified design loading conditions. In this analysis the arm hub was modeled. The outer surfaces of the hub were fixed while a load of 8,957 pounds was applied to one of the splined teeth in order to simulate the design loading conditions. The Model of the hub with the applied loading conditions is shown in Figure 21.

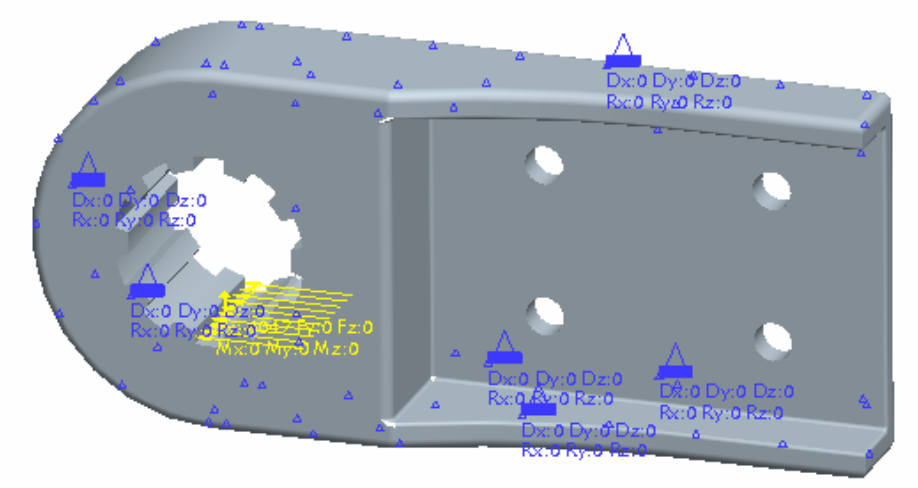

Figure 21 – Static loads applied to hub spline

The results of the finite element analysis of the spline tooth produced from the model shown in Figure 21 generated stresses around 9,500 psi within the tooth. The stress within the spline tooth were within 10 percent of the hand calculations. The Von Mises stress plot for the Pro-Mechanica analysis of splined segment can be found in Appendix A.

7.2 Bolt Pattern Development

Once the spline design for the hub was complete the method of attaching the arm to the hub was considered. The method chosen was to insert the square arm into a sleeve attached to the hub. For ease of alignment and insertion of the arm into the hub a c - shaped sleeve was deemed the best method for arm attachment. The simplest and most reliable method of securing the arm within the hub is to bolt the arm to the hub. The desired bolted connection consisted of four bolts in a 3 inch by 2 inch rectangular pattern. The bolt size was determined using an iterative process based on bolt strength, wall thickness of the arm sleeve attached to the hub, and the thickness of the arm. In order to perform this analysis the forces on the bolts resulting from the normal shear stress of the populated pod and arms combined with the moment created by the pod and arms (illustrated in Figure 22) was determined using the following equations [17]:

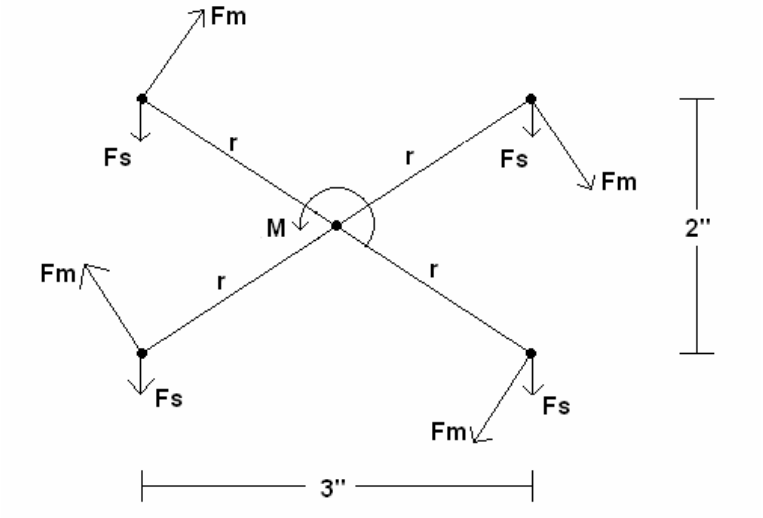

Figure 22 – Bolt loading diagram

$$F_m = \frac{M}{nr} \qquad (8)$$

where

M = moment applied to hub,
r = bolt hole radius from the center of the bolt pattern, and
n = number of bolts.

and

$$F_s = \frac{F}{mn}, \qquad (9)$$

where

F = combined weight of pod and arms,
M = number of arms, and
n = number of bolts.

The total force applied to the bolts is calculated by adding the vectors of the force applied as a result of the moment and the normal shear force applied. The worst case would be when the moment force and the normal shear force act in the same direction thus the resulting bolt force was calculated using the following equation:

$$\overrightarrow{F_b} = \overrightarrow{F_m} + \overrightarrow{F_s}\ . \qquad (10)$$

This resulted in a load of 1,996 pounds that must be carried by each bolt.

7.3 Bolt Sizing

Once the force applied to each bolt as a result of the bolt pattern was determined, the bolt size required to carry the design loading was determined. The following equation was used to calculate the stress applied to each bolt.

$$\tau = \frac{F_b}{A}, \qquad (11)$$

where

A = bolt cross-sectional area and
F_b = force applied to each bolt.

The stress carried by several diameters of bolts was calculated using equation 7 and the results are shown in Table 3.

Table 3 – stress carried by bolts of various sizes

bolt size (in)	tensile area (in^2)	stress on bolt (psi)	Safety Factor SAE Grade 5	Safety Factor SAE Grade 8
3/8	0.09	22733	2.09	2.99
7/16	0.12	16816	2.83	4.04
1/2	0.16	12475	3.82	5.44
9/16	0.20	9833	**4.84**	**6.91**
5/8	0.26	7797	6.11	8.71
3/4	0.37	5351	8.90	12.69

As is shown inTtable 3, all of the bolt sizes considered would support the required loading. For safety reasons it is critical that the bolted connection of the rotational arms to the hubs does not fail. Failure at this point would permit the arms to detach from the sensor platform which could cause damage to the aircraft or objects on the ground below. It is for this reason that a UNC 9/16 SAE grade 5 bolt was deemed to be the most suitable choice for the application at hand.

Although the bolts chosen will sufficiently support the required loading the stresses created on the bolt holes in the arms needed be checked in order to finalize the bolt selection. The bolts generate two different stresses on the bolt holes. The first stress is the bearing stress of the bolt on the hole and was calculated using the following equation:

$$\sigma = \frac{F_b}{A}, \qquad (12)$$

Where

F_b = force applied to each bolt.

and

$$A = td\,, \qquad (13)$$

where

t = wall thickness (thickness of arm) and
d = bolt diameter.

Using a 9/16 inch bolt the resulting bearing stress on the bolt hole was calculated as 4,730 psi. This gave a safety factor of 8.46.

The second stress generated on the bolt hole is that of a shear stress which acts to tear the bolt out of the arm. This stress was calculated was calculated as follows:

$$\tau = \frac{F_b}{A}\,, \qquad (14)$$

where

F_b = force applied to each bolt.

and

$$A = 2tw\,, \qquad (15)$$

where

T = wall thickness (thickness of arm), and
W = distance from the center of the bolt hole to the edge of the arm.

This resulted in a tear out shear stress of 1,331 psi. This resulted in a safety factor of 27.31. From this analysis it was determined that a 9/16 inch bolt would generate sufficiently low stresses within the arm to allow for their use.

In addition to the hand calculations, Pro-Mechanica was also used to analyze the response of the arm bolt holes to the specified design loading conditions. In this analysis the arm end was modeled. The outer edges of the arm were fixed while two separate loads were applied to the arm bolt holes. The first was a load of 94 pounds applied vertically to simulate the normal shear force applied to the bolts via the weight of the

pod, arms, and sensors and the second load was a force of 1,902 pounds applied at an angle of 33.69 degrees from the horizontal axis on each bolt hole to simulate the bolt forces generated by the moment. The model of the arm end with the applied loading conditions is shown in Figure 23.

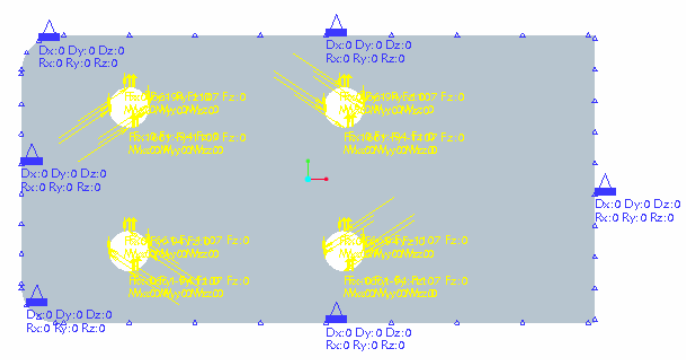

Figure 23 – Static loads applied to arm bolt holes

The results of the finite element analysis of the spline tooth produced from the model shown in Figure 23 generated stresses in the range of 2,500 psi around the bolt holes. The stresses produced in Pro-Mechanica were larger than those calculated for the bolt tear out but smaller than the stresses calculated for the bearing stress. This is most likely because the default mesh size and type applied by Pro-Mechanica do not provide for an accurate representation of the arm behavior under the design loading conditions. Refinement of the mesh properties for the arm model may produce more accurate results. For safety purposes the larger stress results of the hand calculations were considered to be the design stresses. The Von Mises stress plot for the Pro-Mechanica analysis of arm bolt holes can be found in Appendix A.

7.4 Required Sleeve Wall Thickness

In order to determine the required wall thickness for the hub c-section, the same bolt hole analysis performed on the arms was performed on the hub wall. Equations 12

and 14 were rearranged to solve for the required wall thickness which was then calculated to be 0.107 inches. A hub wall thickness of 3/8 inches was chosen which gave a safety factor of 6.91.

In addition to the hand calculations, Pro-Mechanica was also used to analyze the response of the hub bolt holes to the specified design loading conditions. In this analysis the arm – hub was modeled. The individual splined teeth of the hub were fixed while two separate loads were applied to the hub bolt holes. The first was a load of 94 pounds applied vertically to simulate the normal shear force applied to the bolts via the weight of the pod, arms, and sensors and the second load was a force of 1,902 pounds applied at an angle of 33.69 degrees from the horizontal axis on each bolt hole to simulate the bolt forces generated by the moment. The model of the hub with the applied loading conditions is shown in Figure 24.

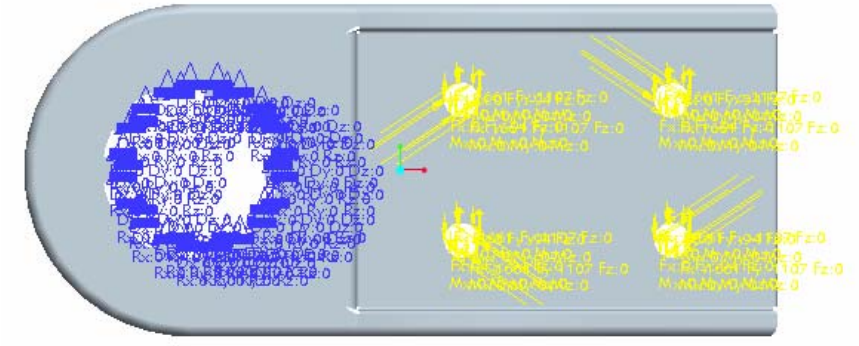

Figure 24 – Static loads applied to arm - hub bolt holes

The results of the finite element analysis of the spline tooth produced from the model shown in Figure 24 generated stresses in the range of 9,000 psi around the bolt holes. The stress around the hub bolt holes were within 10 percent of the hand calculations. The Von Mises stress plot for the Pro-Mechanica analysis of hub bolt holes can be found in Appendix A.

7.5 Hub Design Summary

The geometry of the rotational arm – hub was first determined through the use of hand calculations in order to determine the length of spline engagement required to transmit the torque from the gear reducer to the rotational arms, size the bolts for the mating of the rotational arms to the hub sleeve, and determine the required wall thickness of the arm sleeve section. The hub dimensions based off of the hand calculations were then subjected to a finite element analysis in which the design loading conditions were simulated. The FEA results were used to verify the accuracy of the hand calculations and provide insurance that the finalized hub geometry was structurally sound. The results of both the hand calculations and the finite element analysis are shown in Table 4.

Table 4 – Comparison of hand calculated stress and FEA results

Component	Stress (psi)	FEA Stress (psi)	% Difference Between FEA and Hand Calculations
Splines	8887.57	9500	6.89
Bolts	9828.98	-	-
Hub Bolt Holes	9483.40	9178	3.22
Arm Bolt Holes	4729.56	2500	47.14
Shaft	20690.00	22351	8.03
Shear Key	43334.00	45000	3.84

Examination of Table 4 shows that the hand calculated stresses for each rotational component are close to those produced during the finite element analysis of each component with the exception of the arm bolt holes. The large difference between the

hand calculations of the arm bolt holes and the FEA of the bolt holes was most likely due to the manor in which Pro-Mechanica meshed the solid model of the arm end. Because the hand calculations produced the larger stress values in the arm bolt holes, the hand calculated bolt hole stresses were deemed correct for safety purposes. The final hub design consisted of a circular hub with a cantilevered c-shaped sleeve with a wall thickness of 3/8 inches for which the rotational arms are to be inserted. The arms are secured to the hub sleeve via four SAE UNF 9/16 inch grade 5 bolts. The torque from the rotational shaft is transmitted to the hubs via a standard SAE 10 tooth straight wall spline with a length of spline engagement of 2 inches. The final hub design is shown in Figure 25.

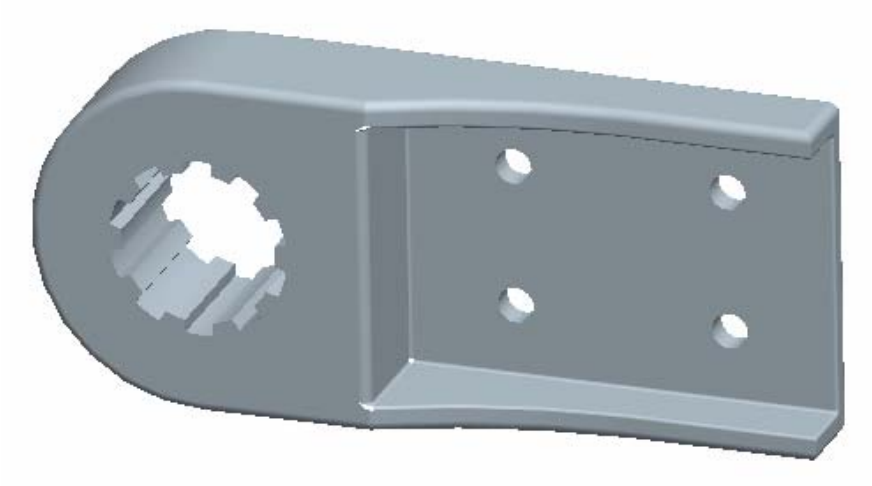

Figure 25 – Final hub design

CHAPTER 8: FATIGUE ANALYSIS

Due to the change in moment arm length from the shaft to the pod/arm structure center of gravity, there is a change in the torque applied to the shaft as the arms rotate. The moment applied to the shaft throughout rotation is shown in Figure 26.

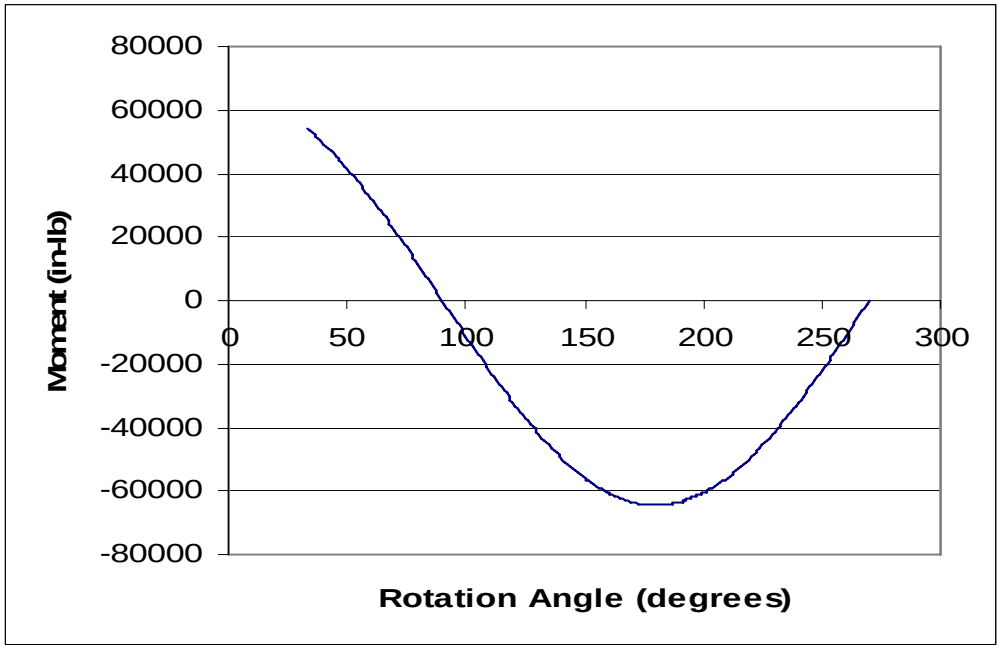

Figure 26 – plot of moment

As a result of this change in loading, i.e. cyclic loading, fatigue is a potential mode of failure for the rotational components. In order to ensure that fatigue will not present a problem in the operation of the rotational system, a modified Goodman analysis was performed for each rotational element studied in the static analysis. In order to perform a modified Goodman analysis the maximum, minimum, and mean stress values of each component throughout the operational cycle must be determined. Figure 26 shows that the maximum and minimum moments occur at 180 degrees and 90 degrees respectively. This maximum moment is equal to 65,000 inch pounds and the minimum

moment is equal to 0 inch pounds. Since the stresses in the rotational elements are directly related to the moment applied to the shaft, they also change with arm position. The stresses of the rotational components with respect to arm position are shown in Figure 27.

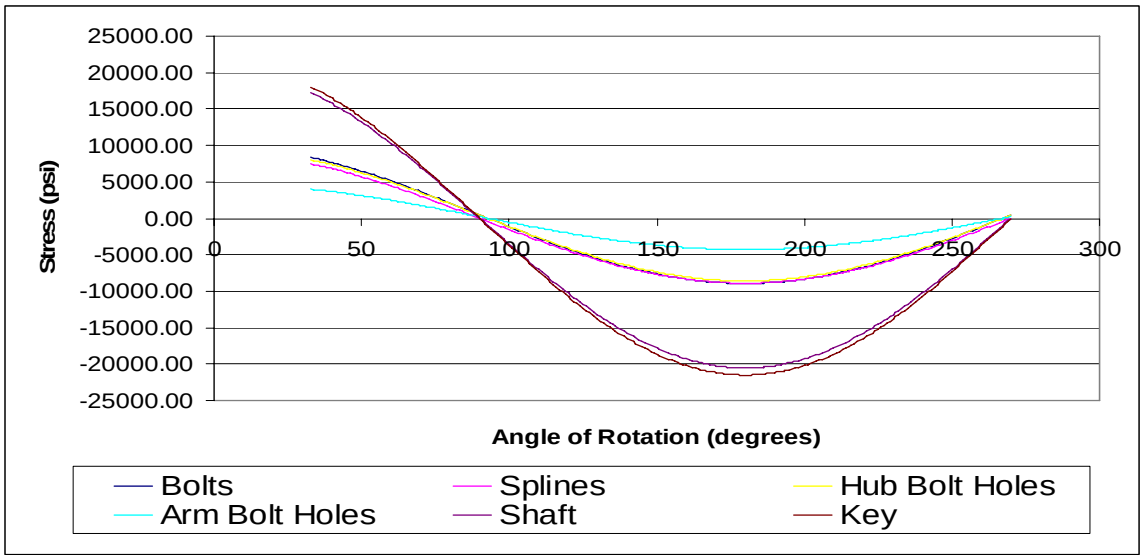

Figure 27 – Plot of rotational component stress during rotation

Calculations for the moment and stresses generated throughout rotation and Goodman diagrams for each rotational component listed in Figure 27 can be found in Appendix B. The maximum, minimum, and mean stress values for each component shown in Figure 27 are listed in Table 5.

Table 5 – Maximum, minimum, and mean stress values

	Bolt Stress (psi)	Spline Stress (psi)	Hub Bolt Hole Stress (psi)	Arm Bolt Hole Stress (psi)	Shaft Stress (psi)	Bearing Key Stress (psi)
Maximum	8317.782	7453.745	8025.332	4002.394	1637.343	17218.74
Minimum	-8905.34	-8887.57	-8592.23	-4285.12	-1753	-20531
Mean	-293.78	-716.91	-283.45	-141.36	-57.83	-1656.13

From Table 5 it is observed that the mean stress values of the components are nonzero, because of this a modified Goodman approach will predict the fatigue analysis accurately. For a life of infinite cycles the maximum modified Goodman stress (S_{max}) must be less than or equal to the yield stress of the component material. The calculation of S_{max} is shown in Equation 16 for a mean stress greater than or equal to zero [12]:

$$S_{\max} = \frac{S_N}{1 - mR}, \qquad (16)$$

where S_N is calculated using Equation 17 or,

$$S_N = 0.5 S_u k . \qquad (17)$$

And k is calculated using Equation 18:

$$k = k_{gr} k_{we} k_f k_{sr} k_{sz} k_{rs} k_{fr} k_{cr} k_{sp} k_r , \qquad (18)$$

Where, k = overall strength influencing factor
k_{gr} = grain size and direction strength influencing factor
k_{we} = welding strength influencing factor
k_f = geometrical discontinuity strength influencing factor
k_{sr} = surface condition strength influencing factor
k_{sz} = size effect strength influencing factor
k_{rs} = residual surface stress strength influencing factor
k_{fr} = fretting strength influencing factor
k_{cr} = corrosion strength influencing factor
k_{sp} = operating speed strength influencing factor
k_r = strength reliability required strength influencing factor

and m is calculated using Equation 19:

$$m = \frac{S_u - S_N}{S_u}, \qquad (19)$$

and R is calculated using Equation 20:

$$R = \frac{\sigma_m}{\sigma_{\max}}, \qquad (20)$$

where σ_m is the mean stress and σ_{max} is the maximum stress value throughout the cycle. Values calculated for S_{max}, S_N, m, and R for each rotational element can be found in Appendix B.

Through the conduction of the fatigue analysis it was evident that all of the rotational element components are capable of withstanding an infinite number of cycles. This is based on the modified Goodman approach which states that if the maximum modified Goodman stress is less than the yield stress for the material the component can withstand an infinite number of rotation cycles (i.e. 10^6 cycles), however, the fatigue results of the rotational system during deployment have not been determined at this time. The results of the fatigue calculations are shown below in Table 6. Fatigue calculations for the remainder of the rotational arms were conducted in a separate analysis prior to the development of the new arm – hub connection. The calculations resulted in an infinite number of rotational life cycles.

Table 6 – Fatigue calculation results

	Max. Stress (psi)	Min. Stress (psi)	Mean Stress (psi)	Ultimate Strength (psi)	Yield Strength (psi)	Max. Modified Goodman Stress (psi)
Spline	7454	-8888	-717	97000	36351	9107
Bolt	8318	-8905	-294	85910	67920	11864
Hub Bolt Hole	8025	-8592	-283	97000	63000	9590
Arm Bolt Hole	4002	-4285	-141	60000	40000	5932
Shaft	1637	-1753	-58	97000	36351	9590
Shear Key	17219	-20531	-1656	97000	36351	9107

CHAPTER 9: RESULTS

The primary goal of this design was to develop a new arm – hub connection configuration for a standardized roll – on, roll – off sensor pallet system for a C – 130 military aircraft. The new hub design was specified to change the arm geometry in such a manor that the stress concentrations at the base of the arm due to the fillet are reduced or eliminated. In addition to reduction of the stress concentrations at the base of the arm, the new hub had to allow for easier assembly and removal of the rotational arms to the hubs for maintenance and manufacturing purposes, and to minimize the backlash in the hub – shaft connection point created by the shear keys in the current hub design. The design of the new hub incorporates a straight sleeve into which the rotational arms are to be inserted. This sleeve serves two purposes. The first purpose is to eliminate the fillet located at the base of the rotational arm, present in the existing arm design. The maximum stress in the current rotational arms is 15,990 psi created by the fillets at the base of the arms. With the new arm – hub design the maximum stress at the base of the arms is reduced to 4,730 psi created by the bolted connection between the arms and the hub. This is a 70 percent reduction in the arm stress around the arm – hub connection region.

The second purpose of the sleeved arm connection is to facilitate easy instillation and removal of the rotational arms to and from the hubs. With the current arm – hub connection, the arms were required to be slid onto the shaft in the same manor as the hubs. While this was not a great concern for initial construction of the sensor pallet, it does present a problem with maintenance of the rotational arms because replacement and servicing of the arms requires disassembly of the entire shaft bearing system. A sleeved

connection allows for the arms to be placed completely outside of the rotational shaft so that the arms can be removed directly from the hubs with no disassembly of the rotational components.

In order to reduce the backlash in the hub – shaft connection point, it was decided to incorporate a standard SAE 10 tooth spline with a class B fit at the new hub – shaft connection point. The class B spline fit allows for ease in the installation of the hub onto the shaft while no load is applied to the system but does not permit any axial translation once a load is applied to the splined connection. The final design of the arm – hub and shaft configuration is shown in Figure 28.

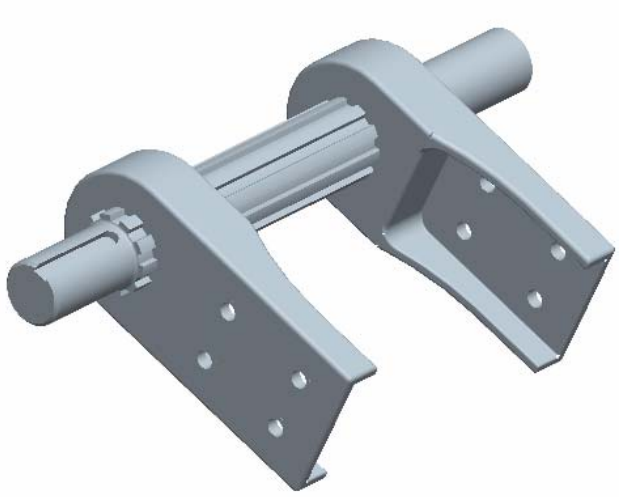

Figure 28 – Final arm – hub and shaft design

The material chosen for the construction of both the arm – hubs and rotational shaft was AISI 4303 steel which has an ultimate tensile strength of 97,000 psi and yield strength of 63,000 psi [18]. The final geometry of the hubs and shaft were based off of these material properties and appropriate safety factors were incorporated into the design. The required hub dimensions were calculated initially by hand and then a finite element analysis was performed on each component to verify the hand calculations. A comparison

of the hand calculations with the FEA results along with the design safety factors for each designed component is listed in Table 7.

Table 7 – FEA - Hand calculated stresses comparison and factor of safety for each rotational component

Component	Stress (psi)	FEA Stress (psi)	% Difference Between FEA and Hand Calculations	Factor of Safety
Splines	8888	9500	6.89	4.09
Bolts	9829	-	-	6.91
Hub Bolt Holes	9483	9178	3.22	6.64
Arm Bolt Holes	4730	2500	47.14	8.46
Shaft	20690	22351	8.03	1.8
Shear Key	43334	45000	3.84	1.45

From Table 7 it can be observed that the lowest factor of safety for the rotational components is 1.45 which occurs within the shear key. This result is desirable because the shear key is the least expensive component in the rotational assembly. By having the lowest factor of safety the shear key will act as a “mechanical fuse” to protect the remainder of the rotational components from failure if the system is exposed to loads in excess of the design conditions. In addition to protecting the remainder of the rotational components from damage, if failure of the shear occurs the rotational components will still remain connected to the sensor platform avoiding a dangerous situation of damage to the aircraft or objects below the aircraft on the ground.

With the design of any component that will undergo cyclic loading, fatigue can present a problem. In order to ensure that failure due to fatigue would not be an issue for the rotational components a modified stress based Goodman analysis was performed on

all of the rotational components. The criteria for the Goodman analysis states that if the maximum modified Goodman stress is less than the yield stress for the material that the component will be able to withstand infinite number of cycles. The results of the modified Goodman analysis are shown in Table 8.

Table 8 – Modified Goodman Analysis Results

Component	Yield Strength (psi)	Max. Modified Goodman Stress (psi)
Spline	36351	17956
Bolt	67920	23098
Hub Bolt Hole	63000	18671
Arm Bolt Hole	40000	11549
Shaft	36351	18671
Shear Key	36351	17956

From Table 8 it can be observed that the maximum Goodman stresses for all of the rotational components are well below the components material yield strength, thus failure due to fatigue is not a problem.

CHAPTER 10: CONCLUSIONS

Upon examination of Table 6 it can be observed that the factors of safety for all of the rotational components, with exception of that for the shear key, seem to be rather conservative. The large safety factors were incorporated because the design loading conditions were based off of assumptions of the actual loading conditions experienced during flight. Because this system is still in the prototype stages, the arm – hub configuration designed in this document will not likely be the final production models.

The next step in order to refine and optimize this design would be to perform an instrumented flight test in which the hubs and arms are fitted with electrical resistance strain gages and accelerometers. The acquisition hardware implemented to receive and record the strain gage and accelerometer data should be capable of recording a real time reading of the behavior of the arms and hubs during the test flight scenarios. The ability to collect the strain gage and accelerometer data in real time will allow for a more accurate development of the actual dynamic loads applied to the rotational system during in flight deployment. With a more accurate design loading model of the arm – hub configuration, it will be possible to perform a further optimization for the hubs and shaft of the current design as well as perform a fatigue analysis on the rotational components to determine if the system will be able to withstand the vibrations present during deployment. In order to ensure that the prototype will survive the flight testing the large safety factors were incorporated into the design of the rotational components.

CHAPTER 11: REFERENCES

[1] Wowczuk, Zenovy S., "Design of a Standardized Sensor Platform for a C-130 Aircraft," Mechanical and Aerospace Engineering Dept., West Virginia University, Morgantown, WV, 26505, Thesis, 2004.

[2] Naternicola, Adam C., "Dynamic Modal Analysis and Optimization of C-130 Project Oculus' Mechanical Arm/Pod Sensor Deployment System Using the Finite Element Method," Mechanical and Aerospace Engineering Dept., West Virginia University, Morgantown, WV, 26505, Thesis, 2004.

[3] Williams, Kenneth A., Zenovy S. Wowczuk, Seth D. Lucey, Kenneth H. Means, James E. Smith, "Hub Connection Simulation of a Sensor Platform System," SAE Paper No. 2005-01-3425.

[4] Wait R., A. R. Mitchel,"Finite Element Analysis and Applications," John Wiley and Sons Ltd., New York 1985.

[5] Brauer, John R. What Every Engineer Should Know About Finite Element Analysis, Marcel Dekker, Inc., New York 1988.

[6] Dubensky, R. G., "What Every Engineer Should Know About Finite Element Analysis Methods," SAE Paper No. 861294.

[7] Guo, Mike and Bhandarkar, Ram and Lin, Barry, "Clamp Load Consideration in Fatigue Life Prediction of a Cast Aluminum Wheel Using Finite Element Analysis," SAE Paper No. 2004-01-1581.

[8] Timoney, S.S. and Timoney, E. P. and Lynch, C., "Correlation of Fatigue Test Results and Finite Element Analysis for a Prototype Independent Suspension Axle Housing," SAE Paper No. 2003-01-3434.

[9] Frost, Colin, "Using Finite Element Analysis Throughout the Product Development Cycle for Plastic Trim Components," SAE Paper No. 950640.

[10] Dharia, Mehul A., "Inserted Tool Design Using Finite Element Analysis," SAE Paper No. 980750.

[11] Wowczuk, Z. S. and Williams, K. and Smith, J. E., "Connection Hub Optimization Using Experimental and Simulated Analysis Results," SEM Paper No. 325.

[12] Collins, Jack A. Mechanical Design of Machine Elements and Machines, John Wiley and Sons, Inc. 2003.

[13] Oberg, Erik, Franklin D. Jones, Holbrook L. Horton, and Henry H. Ryffel. Machinery's Handbook 26th Edition. New York: Industrial Press Inc, 2000.

[14] *Textron Power Transmission*, modelhp/modhp_usa.pdf, Traverse City, MI, 2003 http://www.conedrive.textron.com/download/wormgears.

[15] Pytel, Andrew and Joan Kiusalaas, Engineering Mechanics Dynamics, second edition, Pacific Grove: Brooks/Cole 1999.

[16] Allman III, Robert, "Instructor/Tutor Math and Science," http://www.olysun.com.

[17] Beer, Ferdinand P., and E. Russell Johnston, Jr. Mechanics of Materials. New York: McGraw-Hill Inc, 1992.

[18] Avallone, Eugene A. and Baumeister III, Theodore, Marks' Standard Handbook for Mechanical Engineers, ninth edition, New York: McGraw-Hill 1987.

[19] "Subpart C—Structure," FAR Structural Design Criteria. 26 May 2005.

.

Appendix A

FEA Results for Rotational Components

The following appendix shows the results of the finite element analysis performed on each rotational component with the use of Pro-Mechanica. The colors present in the contour plots of each component represent the Von Mises stress throughout the component under the specified design loading conditions.

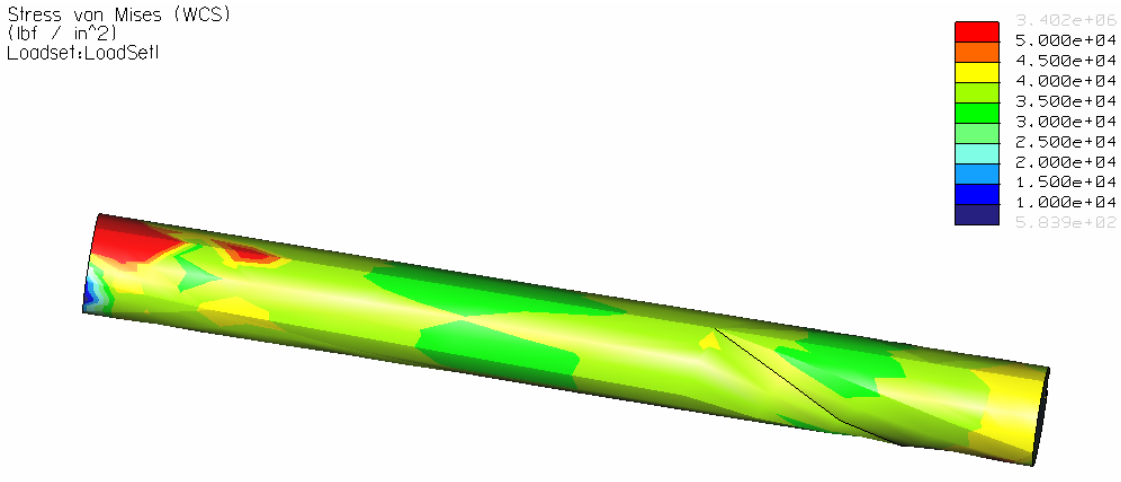

Figure 29 – Von Mises stress generated in shaft using Pro-Mechanica

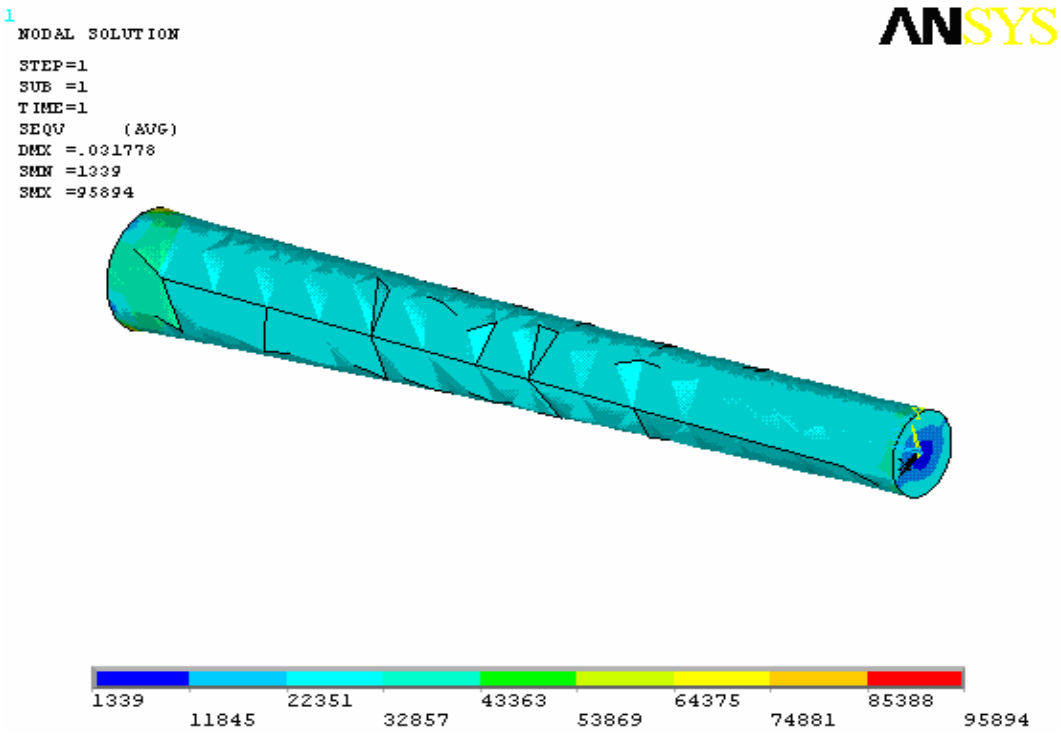

Figure 30 – Von Mises stress generated in shaft using ANSYS

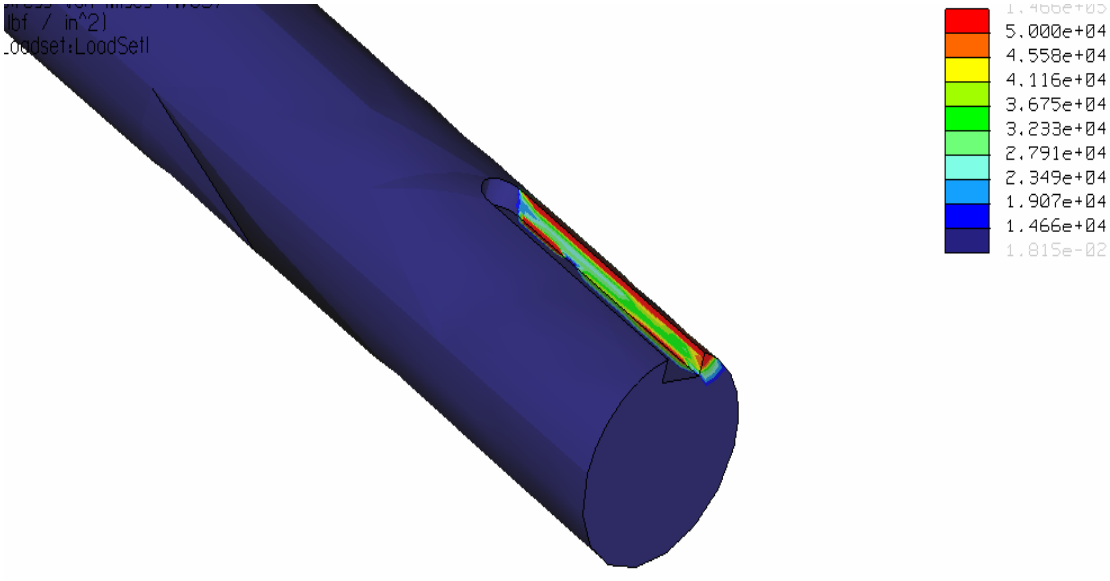

Figure 31 – Von Mises stress generated in shaft keyway

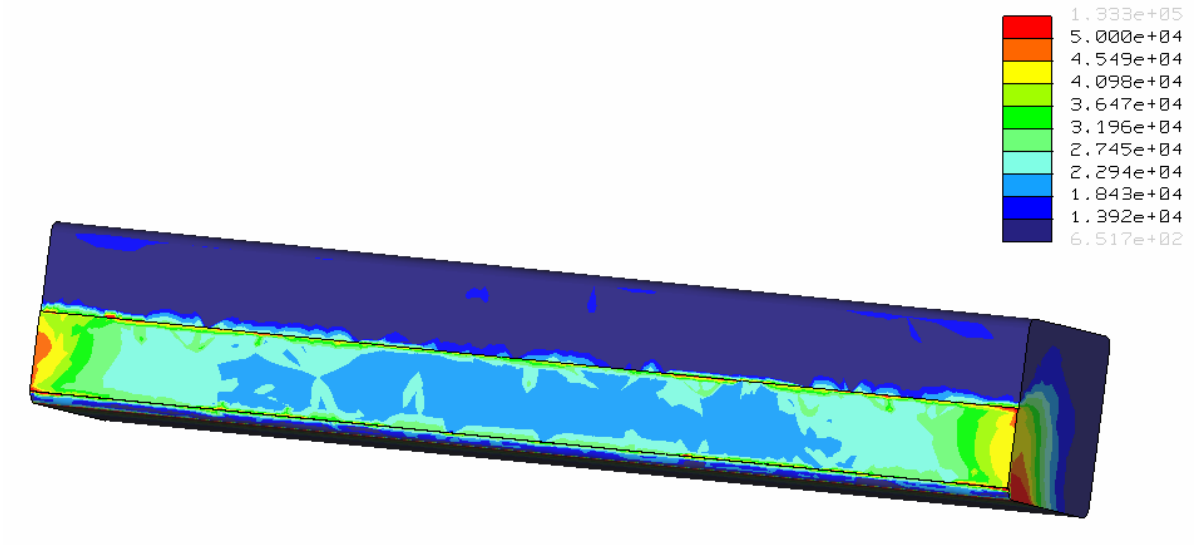

Figure 32 – Von Mises stress generated in shear key

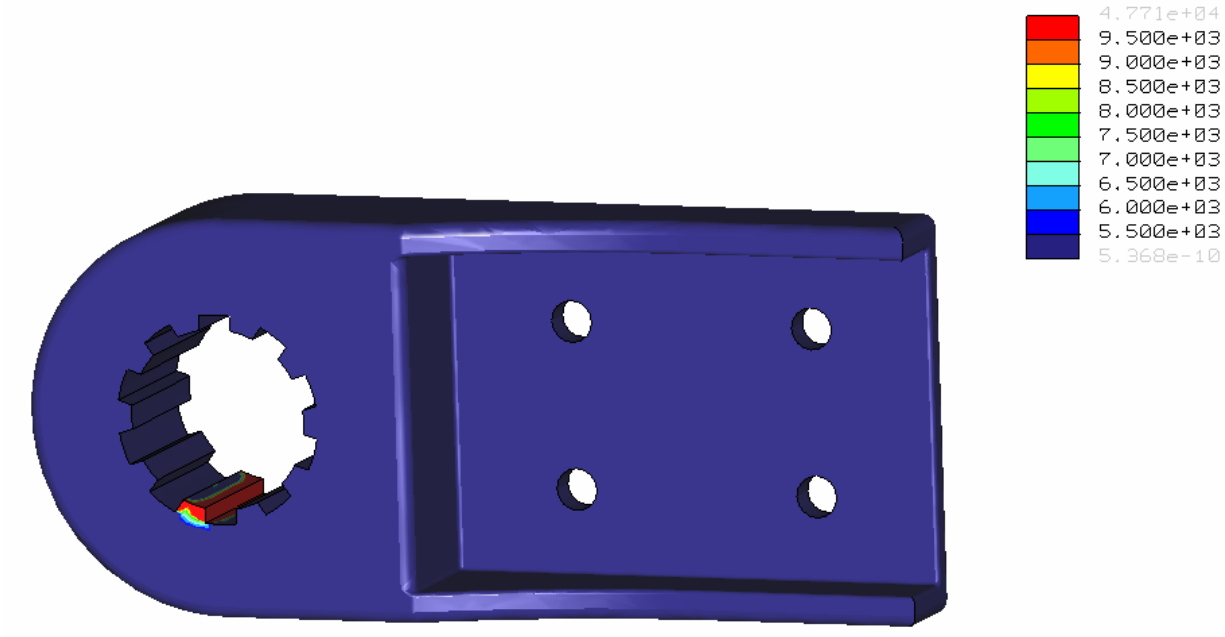

Figure 33 – Von Mises stress generated in splines

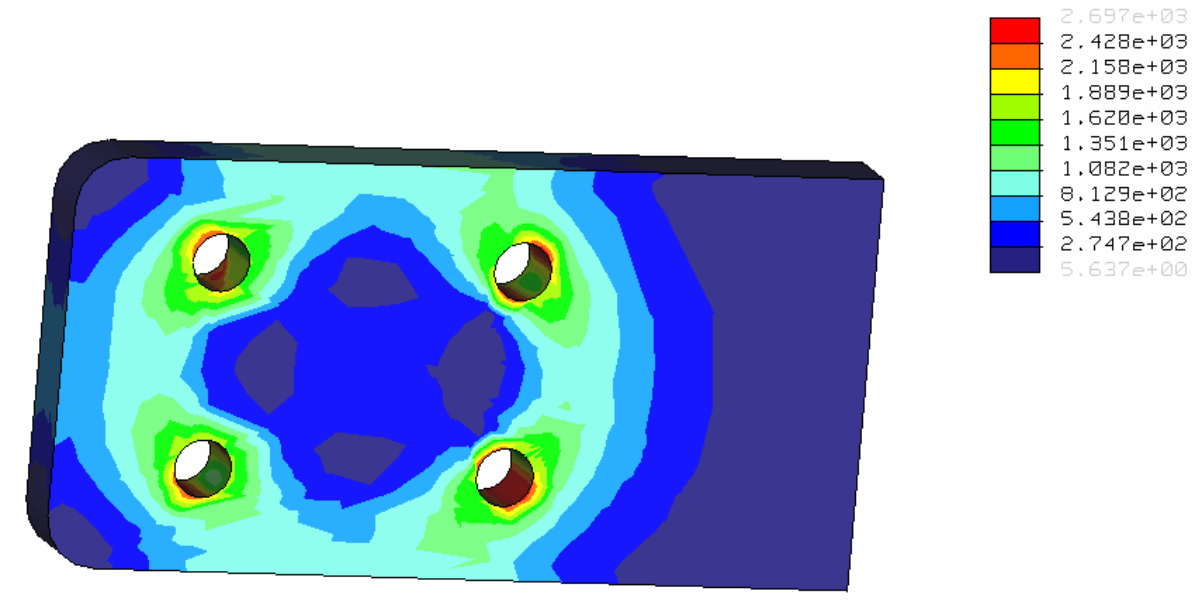

Figure 34 – Von Mises stress generated in arm bolt holes

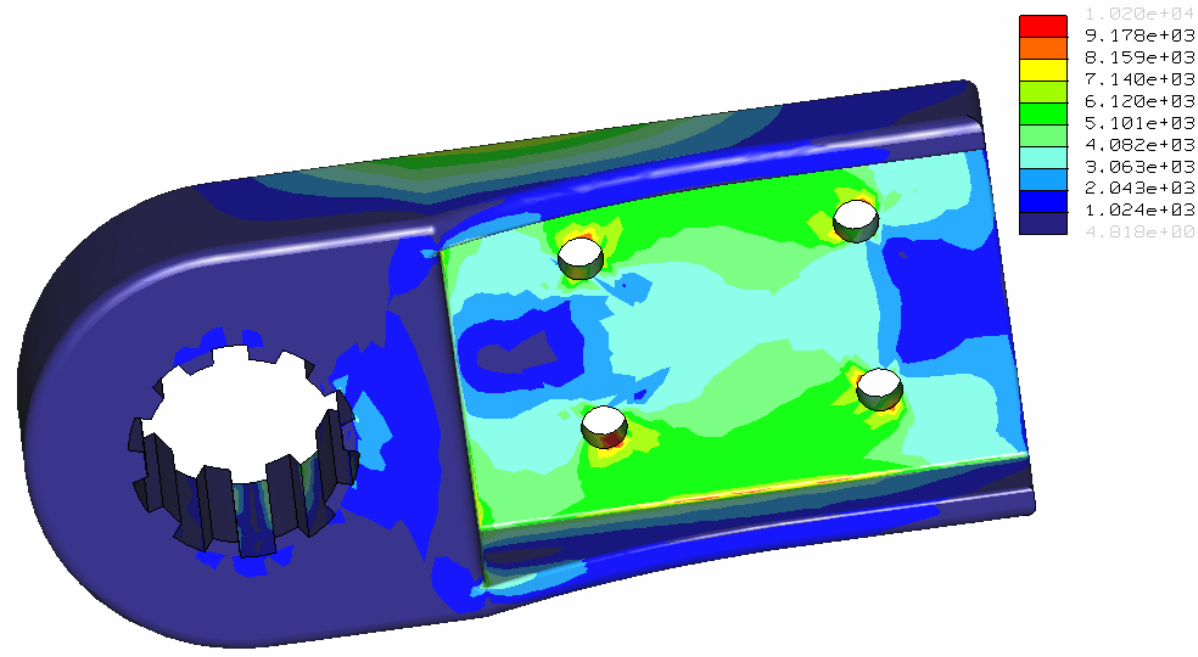

Figure 35 – Von Mises stress generated in hub bolt holes

Appendix B

Fatigue Calculations

and

Goodman Results

Table 9 – Calculation of moment and stresses for each rotational component for each degree of rotation

angle (degrees)	Moment Arm (inches)	Moment (in-lb)	Bolt Stress (psi)	Spline Stress (psi)	Hub Bolt Hole Bearing Stress (psi)	Arm Bolt Hole Bearing Stress (psi)	Hub Bolt Hole Tear-Out Stress (psi)	Arm Bolt Hole Tear-Out Stress (psi)	Shaft Stress (psi)	Shear Key Stress (psi)	Bearing Key Stress (psi)
33	36	54094	8318	7454	8025	4002	1637	1126	17219	18031	36063
34	36	53473	8228	7368	7938	3959	1620	1113	17021	17824	35649
35	35	52835	8135	7280	7849	3914	1601	1101	16818	17612	35224
36	35	52182	8040	7190	7757	3869	1583	1088	16610	17394	34788
37	34	51512	7943	7098	7664	3822	1564	1075	16397	17171	34341
38	34	50827	7843	7004	7567	3774	1544	1061	16179	16942	33884
39	33	50126	7741	6907	7469	3725	1524	1048	15956	16709	33417
40	33	49410	7637	6808	7369	3675	1503	1034	15728	16470	32940
41	32	48679	7531	6708	7267	3624	1483	1019	15495	16226	32453
42	32	47933	7423	6605	7162	3572	1461	1005	15257	15978	31955
43	31	47172	7313	6500	7055	3519	1439	990	15015	15724	31448
44	31	46397	7200	6393	6947	3465	1417	974	14769	15466	30932
45	30	45608	7085	6284	6836	3409	1395	959	14518	15203	30406
46	30	44805	6969	6174	6724	3353	1372	943	14262	14935	29870
47	29	43989	6850	6061	6609	3296	1348	927	14002	14663	29326
48	29	43159	6730	5947	6493	3238	1325	911	13738	14386	28773
49	28	42316	6607	5831	6375	3179	1301	894	13470	14105	28211
50	28	41460	6483	5713	6255	3119	1276	877	13197	13820	27640
51	27	40591	6357	5593	6133	3059	1251	860	12921	13530	27061
52	26	39710	6229	5472	6010	2997	1226	843	12640	13237	26473
53	26	38817	6099	5349	5885	2935	1201	825	12356	12939	25878
54	25	37912	5968	5224	5758	2872	1175	808	12068	12637	25275

55	25	36996	5835	5098	5629	2808	1149	790	11776	12332	24664
56	24	36068	5700	4970	5499	2743	1122	771	11481	12023	24045
57	23	35129	5564	4841	5368	2677	1095	753	11182	11710	23419
58	23	34180	5426	4710	5235	2611	1068	734	10880	11393	22787
59	22	33220	5286	4577	5100	2544	1041	715	10574	11073	22147
60	22	32250	5145	4444	4964	2476	1013	696	10265	10750	21500
61	21	31270	5003	4309	4827	2407	985	677	9954	10423	20847
62	20	30281	4859	4172	4689	2338	957	658	9639	10094	20187
63	20	29282	4714	4035	4549	2269	928	638	9321	9761	19522
64	19	28275	4568	3896	4408	2198	899	618	9000	9425	18850
65	18	27259	4421	3756	4265	2127	870	598	8677	9086	18173
66	17	26235	4272	3615	4122	2056	841	578	8351	8745	17490
67	17	25202	4122	3473	3977	1983	811	558	8022	8401	16801
68	16	24162	3971	3329	3831	1911	782	537	7691	8054	16108
69	15	23115	3819	3185	3684	1838	752	517	7358	7705	15410
70	15	22060	3666	3040	3537	1764	722	496	7022	7353	14707
71	14	20999	3511	2894	3388	1690	691	475	6684	7000	13999
72	13	19932	3356	2746	3238	1615	661	454	6344	6644	13288
73	13	18858	3201	2598	3088	1540	630	433	6003	6286	12572
74	12	17779	3044	2450	2937	1465	599	412	5659	5926	11852
75	11	16694	2886	2300	2785	1389	568	391	5314	5565	11129
76	10	15604	2728	2150	2632	1313	537	369	4967	5201	10403
77	10	14509	2569	1999	2479	1236	506	348	4618	4836	9673
78	9	13410	2409	1848	2325	1159	474	326	4269	4470	8940
79	8	12307	2249	1696	2170	1082	443	304	3917	4102	8205
80	7	11200	2088	1543	2015	1005	411	283	3565	3733	7467
81	7	10090	1927	1390	1859	927	379	261	3212	3363	6727
82	6	8977	1765	1237	1703	850	348	239	2857	2992	5984
83	5	7861	1603	1083	1547	772	316	217	2502	2620	5240
84	4	6742	1441	929	1390	693	284	195	2146	2247	4495
85	4	5622	1278	775	1233	615	252	173	1789	1874	3748
86	3	4499	1115	620	1076	537	220	151	1432	1500	3000

87	2	3376	952	465	919	458	187	129	1075	1125	2250
88	2	2251	789	310	761	380	155	107	717	750	1501
89	1	1126	625	155	603	301	123	85	358	375	750
90	0	0	462	0	446	222	91	63	0	0	0
91	-1	-1126	298	-155	288	144	59	40	-358	-375	-750
92	-2	-2251	135	-310	130	65	27	18	-717	-750	-1501
93	-2	-3376	-28	-465	-27	-14	-6	-4	-1075	-1125	-2250
94	-3	-4499	-192	-620	-185	-92	-38	-26	-1432	-1500	-3000
95	-4	-5622	-355	-775	-342	-171	-70	-48	-1789	-1874	-3748
96	-4	-6742	-517	-929	-499	-249	-102	-70	-2146	-2247	-4495
97	-5	-7861	-680	-1083	-656	-327	-134	-92	-2502	-2620	-5240
98	-6	-8977	-842	-1237	-812	-405	-166	-114	-2857	-2992	-5984
99	-7	-10090	-1004	-1390	-968	-483	-198	-136	-3212	-3363	-6727
100	-7	-11200	-1165	-1543	-1124	-560	-229	-158	-3565	-3733	-7467
101	-8	-12307	-1326	-1696	-1279	-638	-261	-179	-3917	-4102	-8205
102	-9	-13410	-1486	-1848	-1433	-715	-292	-201	-4269	-4470	-8940
103	-10	-14509	-1645	-1999	-1587	-792	-324	-223	-4618	-4836	-9673
104	-10	-15604	-1804	-2150	-1741	-868	-355	-244	-4967	-5201	-10403
105	-11	-16694	-1963	-2300	-1894	-944	-386	-266	-5314	-5565	-11129
106	-12	-17779	-2120	-2450	-2046	-1020	-417	-287	-5659	-5926	-11852
107	-13	-18858	-2277	-2598	-2197	-1096	-448	-308	-6003	-6286	-12572
108	-13	-19932	-2433	-2746	-2347	-1171	-479	-329	-6344	-6644	-13288
109	-14	-20999	-2588	-2894	-2497	-1245	-509	-350	-6684	-7000	-13999
110	-15	-22060	-2742	-3040	-2646	-1319	-540	-371	-7022	-7353	-14707
111	-15	-23115	-2895	-3185	-2793	-1393	-570	-392	-7358	-7705	-15410
112	-16	-24162	-3047	-3329	-2940	-1466	-600	-412	-7691	-8054	-16108
113	-17	-25202	-3198	-3473	-3086	-1539	-630	-433	-8022	-8401	-16801
114	-17	-26235	-3348	-3615	-3230	-1611	-659	-453	-8351	-8745	-17490
115	-18	-27259	-3497	-3756	-3374	-1683	-688	-473	-8677	-9086	-18173
116	-19	-28275	-3644	-3896	-3516	-1754	-717	-493	-9000	-9425	-18850
117	-20	-29282	-3791	-4035	-3657	-1824	-746	-513	-9321	-9761	-19522
118	-20	-30281	-3936	-4172	-3797	-1894	-775	-533	-9639	-10094	-20187

119	-21	-31270	-4079	-4309	-3936	-1963	-803	-552	-9954	-10423	-20847
120	-22	-32250	-4222	-4444	-4073	-2031	-831	-571	-10265	-10750	-21500
121	-22	-33220	-4363	-4577	-4209	-2099	-859	-590	-10574	-11073	-22147
122	-23	-34180	-4502	-4710	-4344	-2166	-886	-609	-10880	-11393	-22787
123	-23	-35129	-4640	-4841	-4477	-2233	-913	-628	-11182	-11710	-23419
124	-24	-36068	-4776	-4970	-4608	-2298	-940	-646	-11481	-12023	-24045
125	-25	-36996	-4911	-5098	-4738	-2363	-967	-665	-11776	-12332	-24664
126	-25	-37912	-5044	-5224	-4867	-2427	-993	-683	-12068	-12637	-25275
127	-26	-38817	-5175	-5349	-4994	-2490	-1019	-700	-12356	-12939	-25878
128	-26	-39710	-5305	-5472	-5119	-2553	-1044	-718	-12640	-13237	-26473
129	-27	-40591	-5433	-5593	-5242	-2614	-1070	-735	-12921	-13530	-27061
130	-28	-41460	-5559	-5713	-5364	-2675	-1094	-752	-13197	-13820	-27640
131	-28	-42316	-5684	-5831	-5484	-2735	-1119	-769	-13470	-14105	-28211
132	-29	-43159	-5806	-5947	-5602	-2794	-1143	-786	-13738	-14386	-28773
133	-29	-43989	-5927	-6061	-5718	-2852	-1167	-802	-14002	-14663	-29326
134	-30	-44805	-6045	-6174	-5833	-2909	-1190	-818	-14262	-14935	-29870
135	-30	-45608	-6162	-6284	-5945	-2965	-1213	-834	-14518	-15203	-30406
136	-31	-46397	-6276	-6393	-6056	-3020	-1235	-849	-14769	-15466	-30932
137	-31	-47172	-6389	-6500	-6164	-3074	-1258	-865	-15015	-15724	-31448
138	-32	-47933	-6499	-6605	-6271	-3127	-1279	-880	-15257	-15978	-31955
139	-32	-48679	-6608	-6708	-6375	-3180	-1301	-894	-15495	-16226	-32453
140	-33	-49410	-6714	-6808	-6478	-3231	-1322	-909	-15728	-16470	-32940
141	-33	-50126	-6818	-6907	-6578	-3281	-1342	-923	-15956	-16709	-33417
142	-34	-50827	-6920	-7004	-6676	-3330	-1362	-936	-16179	-16942	-33884
143	-34	-51512	-7019	-7098	-6772	-3377	-1382	-950	-16397	-17171	-34341
144	-35	-52182	-7116	-7190	-6866	-3424	-1401	-963	-16610	-17394	-34788
145	-35	-52835	-7211	-7280	-6958	-3470	-1420	-976	-16818	-17612	-35224
146	-36	-53473	-7304	-7368	-7047	-3515	-1438	-988	-17021	-17824	-35649
147	-36	-54094	-7394	-7454	-7134	-3558	-1456	-1001	-17219	-18031	-36063
148	-36	-54699	-7482	-7537	-7219	-3600	-1473	-1013	-17411	-18233	-36466
149	-37	-55287	-7567	-7618	-7301	-3641	-1490	-1024	-17598	-18429	-36858
150	-37	-55859	-7650	-7697	-7381	-3681	-1506	-1035	-17780	-18620	-37239

151	-38	-56413	-7731	-7773	-7459	-3720	-1522	-1046	-17957	-18804	-37609
152	-38	-56950	-7809	-7847	-7534	-3758	-1537	-1057	-18128	-18983	-37967
153	-38	-57470	-7884	-7919	-7607	-3794	-1552	-1067	-18293	-19157	-38313
154	-39	-57972	-7957	-7988	-7678	-3829	-1566	-1077	-18453	-19324	-38648
155	-39	-58457	-8028	-8055	-7745	-3863	-1580	-1086	-18607	-19486	-38971
156	-39	-58924	-8096	-8119	-7811	-3895	-1594	-1096	-18756	-19641	-39282
157	-40	-59373	-8161	-8181	-7874	-3927	-1606	-1104	-18899	-19791	-39582
158	-40	-59803	-8223	-8240	-7934	-3957	-1619	-1113	-19036	-19934	-39869
159	-40	-60216	-8283	-8297	-7992	-3986	-1631	-1121	-19167	-20072	-40144
160	-40	-60610	-8340	-8352	-8047	-4013	-1642	-1129	-19293	-20203	-40407
161	-41	-60986	-8395	-8403	-8100	-4040	-1653	-1136	-19412	-20329	-40657
162	-41	-61343	-8447	-8453	-8150	-4065	-1663	-1143	-19526	-20448	-40895
163	-41	-61682	-8496	-8499	-8197	-4088	-1672	-1150	-19634	-20561	-41121
164	-41	-62001	-8542	-8543	-8242	-4111	-1682	-1156	-19736	-20667	-41334
165	-42	-62302	-8586	-8585	-8284	-4132	-1690	-1162	-19831	-20767	-41535
166	-42	-62584	-8627	-8624	-8324	-4151	-1698	-1168	-19921	-20861	-41723
167	-42	-62847	-8665	-8660	-8361	-4170	-1706	-1173	-20005	-20949	-41898
168	-42	-63091	-8701	-8693	-8395	-4187	-1713	-1177	-20082	-21030	-42060
169	-42	-63315	-8733	-8724	-8426	-4202	-1719	-1182	-20154	-21105	-42210
170	-42	-63520	-8763	-8753	-8455	-4217	-1725	-1186	-20219	-21173	-42347
171	-42	-63706	-8790	-8778	-8481	-4230	-1730	-1190	-20278	-21235	-42471
172	-43	-63872	-8814	-8801	-8504	-4241	-1735	-1193	-20331	-21291	-42582
173	-43	-64019	-8836	-8821	-8525	-4252	-1739	-1196	-20378	-21340	-42679
174	-43	-64147	-8854	-8839	-8543	-4260	-1743	-1198	-20419	-21382	-42764
175	-43	-64255	-8870	-8854	-8558	-4268	-1746	-1200	-20453	-21418	-42836
176	-43	-64343	-8883	-8866	-8570	-4274	-1749	-1202	-20481	-21448	-42895
177	-43	-64412	-8892	-8875	-8580	-4279	-1750	-1203	-20503	-21471	-42941
178	-43	-64461	-8900	-8882	-8587	-4282	-1752	-1204	-20518	-21487	-42974
179	-43	-64490	-8904	-8886	-8591	-4284	-1753	-1205	-20528	-21497	-42993
180	-43	-64500	-8905	-8888	-8592	-4285	-1753	-1205	-20531	-21500	-43000
181	-43	-64490	-8904	-8886	-8591	-4284	-1753	-1205	-20528	-21497	-42993
182	-43	-64461	-8900	-8882	-8587	-4282	-1752	-1204	-20518	-21487	-42974

183	-43	-64412	-8892	-8875	-8580	-4279	-1750	-1203	-20503	-21471	-42941
184	-43	-64343	-8883	-8866	-8570	-4274	-1749	-1202	-20481	-21448	-42895
185	-43	-64255	-8870	-8854	-8558	-4268	-1746	-1200	-20453	-21418	-42836
186	-43	-64147	-8854	-8839	-8543	-4260	-1743	-1198	-20419	-21382	-42764
187	-43	-64019	-8836	-8821	-8525	-4252	-1739	-1196	-20378	-21340	-42679
188	-43	-63872	-8814	-8801	-8504	-4241	-1735	-1193	-20331	-21291	-42582
189	-42	-63706	-8790	-8778	-8481	-4230	-1730	-1190	-20278	-21235	-42471
190	-42	-63520	-8763	-8753	-8455	-4217	-1725	-1186	-20219	-21173	-42347
191	-42	-63315	-8733	-8724	-8426	-4202	-1719	-1182	-20154	-21105	-42210
192	-42	-63091	-8701	-8693	-8395	-4187	-1713	-1177	-20082	-21030	-42060
193	-42	-62847	-8665	-8660	-8361	-4170	-1706	-1173	-20005	-20949	-41898
194	-42	-62584	-8627	-8624	-8324	-4151	-1698	-1168	-19921	-20861	-41723
195	-42	-62302	-8586	-8585	-8284	-4132	-1690	-1162	-19831	-20767	-41535
196	-41	-62001	-8542	-8543	-8242	-4111	-1682	-1156	-19736	-20667	-41334
197	-41	-61682	-8496	-8499	-8197	-4088	-1672	-1150	-19634	-20561	-41121
198	-41	-61343	-8447	-8453	-8150	-4065	-1663	-1143	-19526	-20448	-40895
199	-41	-60986	-8395	-8403	-8100	-4040	-1653	-1136	-19412	-20329	-40657
200	-40	-60610	-8340	-8352	-8047	-4013	-1642	-1129	-19293	-20203	-40407
201	-40	-60216	-8283	-8297	-7992	-3986	-1631	-1121	-19167	-20072	-40144
202	-40	-59803	-8223	-8240	-7934	-3957	-1619	-1113	-19036	-19934	-39869
203	-40	-59373	-8161	-8181	-7874	-3927	-1606	-1104	-18899	-19791	-39582
204	-39	-58924	-8096	-8119	-7811	-3895	-1594	-1096	-18756	-19641	-39282
205	-39	-58457	-8028	-8055	-7745	-3863	-1580	-1086	-18607	-19486	-38971
206	-39	-57972	-7957	-7988	-7678	-3829	-1566	-1077	-18453	-19324	-38648
207	-38	-57470	-7884	-7919	-7607	-3794	-1552	-1067	-18293	-19157	-38313
208	-38	-56950	-7809	-7847	-7534	-3758	-1537	-1057	-18128	-18983	-37967
209	-38	-56413	-7731	-7773	-7459	-3720	-1522	-1046	-17957	-18804	-37609
210	-37	-55859	-7650	-7697	-7381	-3681	-1506	-1035	-17780	-18620	-37239
211	-37	-55287	-7567	-7618	-7301	-3641	-1490	-1024	-17598	-18429	-36858
212	-36	-54699	-7482	-7537	-7219	-3600	-1473	-1013	-17411	-18233	-36466
213	-36	-54094	-7394	-7454	-7134	-3558	-1456	-1001	-17219	-18031	-36063
214	-36	-53473	-7304	-7368	-7047	-3515	-1438	-988	-17021	-17824	-35649

215	-35	-52835	-7211	-7280	-6958	-3470	-1420	-976	-16818	-17612	-35224
216	-35	-52182	-7116	-7190	-6866	-3424	-1401	-963	-16610	-17394	-34788
217	-34	-51512	-7019	-7098	-6772	-3377	-1382	-950	-16397	-17171	-34341
218	-34	-50827	-6920	-7004	-6676	-3330	-1362	-936	-16179	-16942	-33884
219	-33	-50126	-6818	-6907	-6578	-3281	-1342	-923	-15956	-16709	-33417
220	-33	-49410	-6714	-6808	-6478	-3231	-1322	-909	-15728	-16470	-32940
221	-32	-48679	-6608	-6708	-6375	-3180	-1301	-894	-15495	-16226	-32453
222	-32	-47933	-6499	-6605	-6271	-3127	-1279	-880	-15257	-15978	-31955
223	-31	-47172	-6389	-6500	-6164	-3074	-1258	-865	-15015	-15724	-31448
224	-31	-46397	-6276	-6393	-6056	-3020	-1235	-849	-14769	-15466	-30932
225	-30	-45608	-6162	-6284	-5945	-2965	-1213	-834	-14518	-15203	-30406
226	-30	-44805	-6045	-6174	-5833	-2909	-1190	-818	-14262	-14935	-29870
227	-29	-43989	-5927	-6061	-5718	-2852	-1167	-802	-14002	-14663	-29326
228	-29	-43159	-5806	-5947	-5602	-2794	-1143	-786	-13738	-14386	-28773
229	-28	-42316	-5684	-5831	-5484	-2735	-1119	-769	-13470	-14105	-28211
230	-28	-41460	-5559	-5713	-5364	-2675	-1094	-752	-13197	-13820	-27640
231	-27	-40591	-5433	-5593	-5242	-2614	-1070	-735	-12921	-13530	-27061
232	-26	-39710	-5305	-5472	-5119	-2553	-1044	-718	-12640	-13237	-26473
233	-26	-38817	-5175	-5349	-4994	-2490	-1019	-700	-12356	-12939	-25878
234	-25	-37912	-5044	-5224	-4867	-2427	-993	-683	-12068	-12637	-25275
235	-25	-36996	-4911	-5098	-4738	-2363	-967	-665	-11776	-12332	-24664
236	-24	-36068	-4776	-4970	-4608	-2298	-940	-646	-11481	-12023	-24045
237	-23	-35129	-4640	-4841	-4477	-2233	-913	-628	-11182	-11710	-23419
238	-23	-34180	-4502	-4710	-4344	-2166	-886	-609	-10880	-11393	-22787
239	-22	-33220	-4363	-4577	-4209	-2099	-859	-590	-10574	-11073	-22147
240	-22	-32250	-4222	-4444	-4073	-2031	-831	-571	-10265	-10750	-21500
241	-21	-31270	-4079	-4309	-3936	-1963	-803	-552	-9954	-10423	-20847
242	-20	-30281	-3936	-4172	-3797	-1894	-775	-533	-9639	-10094	-20187
243	-20	-29282	-3791	-4035	-3657	-1824	-746	-513	-9321	-9761	-19522
244	-19	-28275	-3644	-3896	-3516	-1754	-717	-493	-9000	-9425	-18850
245	-18	-27259	-3497	-3756	-3374	-1683	-688	-473	-8677	-9086	-18173
246	-17	-26235	-3348	-3615	-3230	-1611	-659	-453	-8351	-8745	-17490

247	-17	-25202	-3198	-3473	-3086	-1539	-630	-433	-8022	-8401	-16801
248	-16	-24162	-3047	-3329	-2940	-1466	-600	-412	-7691	-8054	-16108
249	-15	-23115	-2895	-3185	-2793	-1393	-570	-392	-7358	-7705	-15410
250	-15	-22060	-2742	-3040	-2646	-1319	-540	-371	-7022	-7353	-14707
251	-14	-20999	-2588	-2894	-2497	-1245	-509	-350	-6684	-7000	-13999
252	-13	-19932	-2433	-2746	-2347	-1171	-479	-329	-6344	-6644	-13288
253	-13	-18858	-2277	-2598	-2197	-1096	-448	-308	-6003	-6286	-12572
254	-12	-17779	-2120	-2450	-2046	-1020	-417	-287	-5659	-5926	-11852
255	-11	-16694	-1963	-2300	-1894	-944	-386	-266	-5314	-5565	-11129
256	-10	-15604	-1804	-2150	-1741	-868	-355	-244	-4967	-5201	-10403
257	-10	-14509	-1645	-1999	-1587	-792	-324	-223	-4618	-4836	-9673
258	-9	-13410	-1486	-1848	-1433	-715	-292	-201	-4269	-4470	-8940
259	-8	-12307	-1326	-1696	-1279	-638	-261	-179	-3917	-4102	-8205
260	-7	-11200	-1165	-1543	-1124	-560	-229	-158	-3565	-3733	-7467
261	-7	-10090	-1004	-1390	-968	-483	-198	-136	-3212	-3363	-6727
262	-6	-8977	-842	-1237	-812	-405	-166	-114	-2857	-2992	-5984
263	-5	-7861	-680	-1083	-656	-327	-134	-92	-2502	-2620	-5240
264	-4	-6742	-517	-929	-499	-249	-102	-70	-2146	-2247	-4495
265	-4	-5622	-355	-775	-342	-171	-70	-48	-1789	-1874	-3748
266	-3	-4499	-192	-620	-185	-92	-38	-26	-1432	-1500	-3000
267	-2	-3376	-28	-465	-27	-14	-6	-4	-1075	-1125	-2250
268	-2	-2251	135	-310	130	65	27	18	-717	-750	-1501
269	-1	-1126	298	-155	288	144	59	40	-358	-375	-750
270	0	0	462	0	446	222	91	62	0	0	0

Table 10 – Modified Goodman calculation results for each rotational component

	Bolt	Spline	Hub Bolt Hole	Arm Bolt Hole	Shaft Stress (psi)	Key Stress (psi)
s_f	12240	9894	9894	6120	9894	9894
m	0.90	0.90	0.90	0.90	0.90	0.90
R	0.52	0.50	0.52	0.52	0.52	0.50
S_{max} (psi)	23099	17956	18671	11549	18671	17956

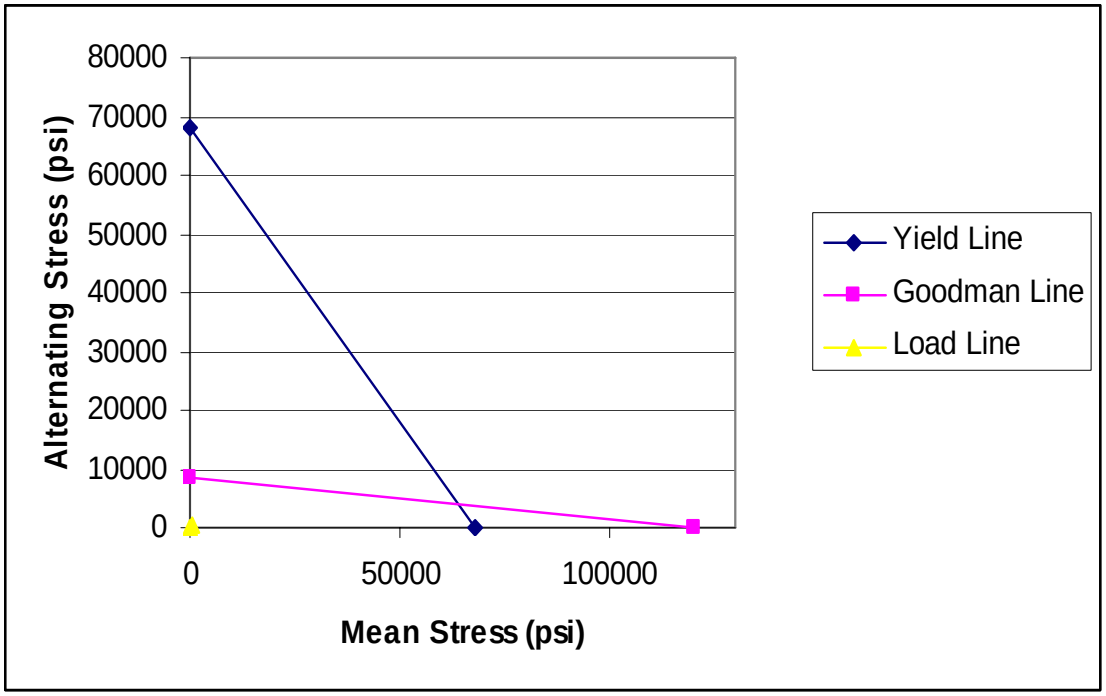

Figure 36 – Bolt Goodman diagram

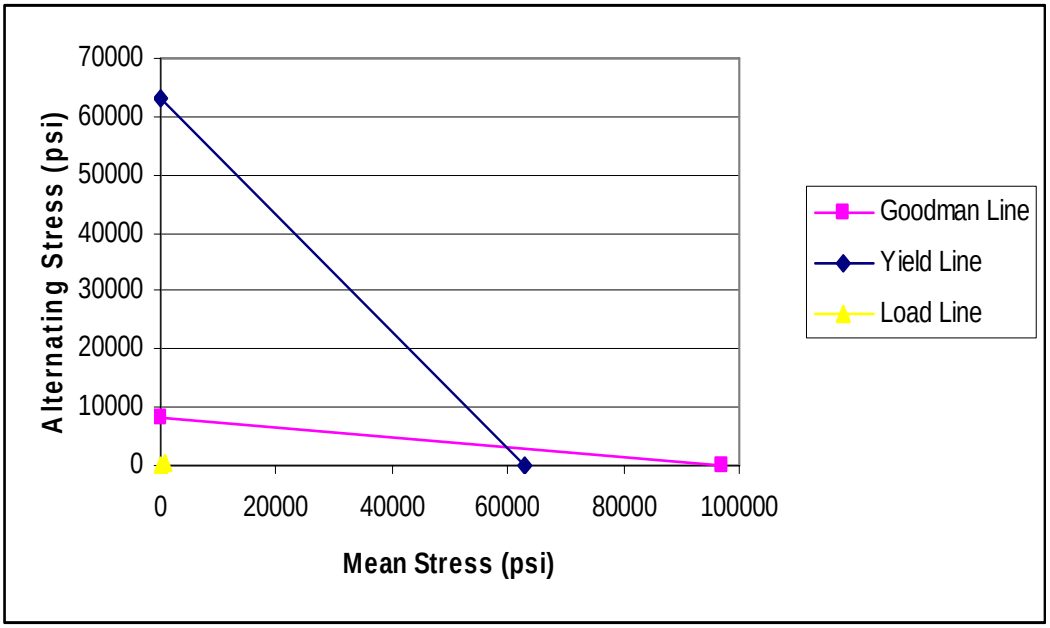

Figure 37 – Spline Goodman diagram

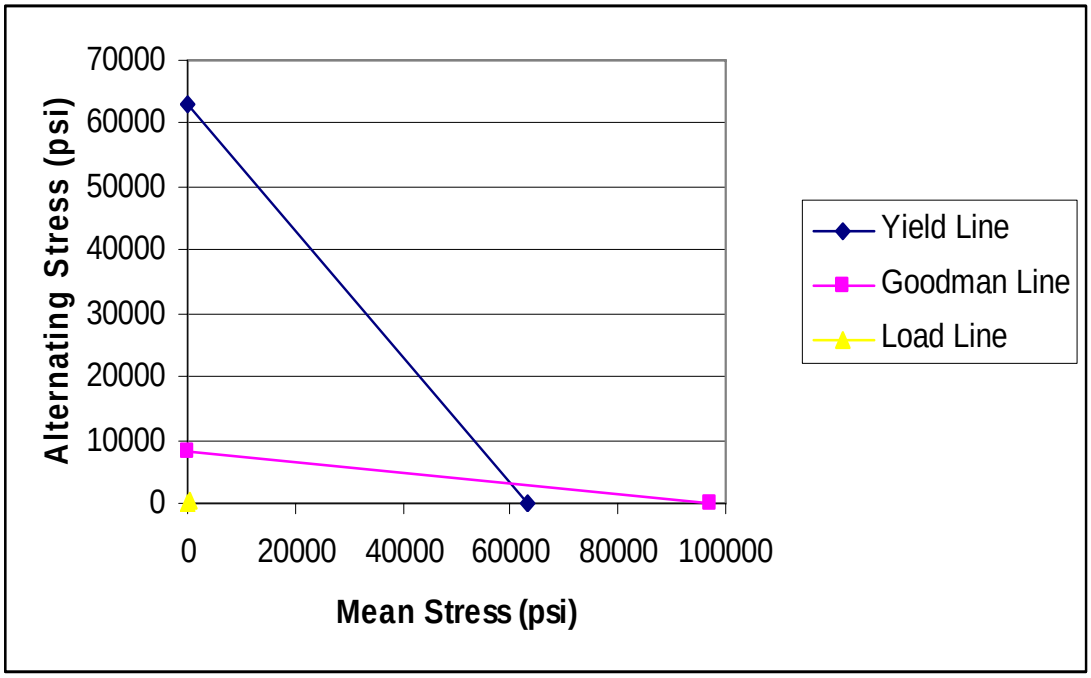

Figure 38 – Hub bolt hole Goodman diagram

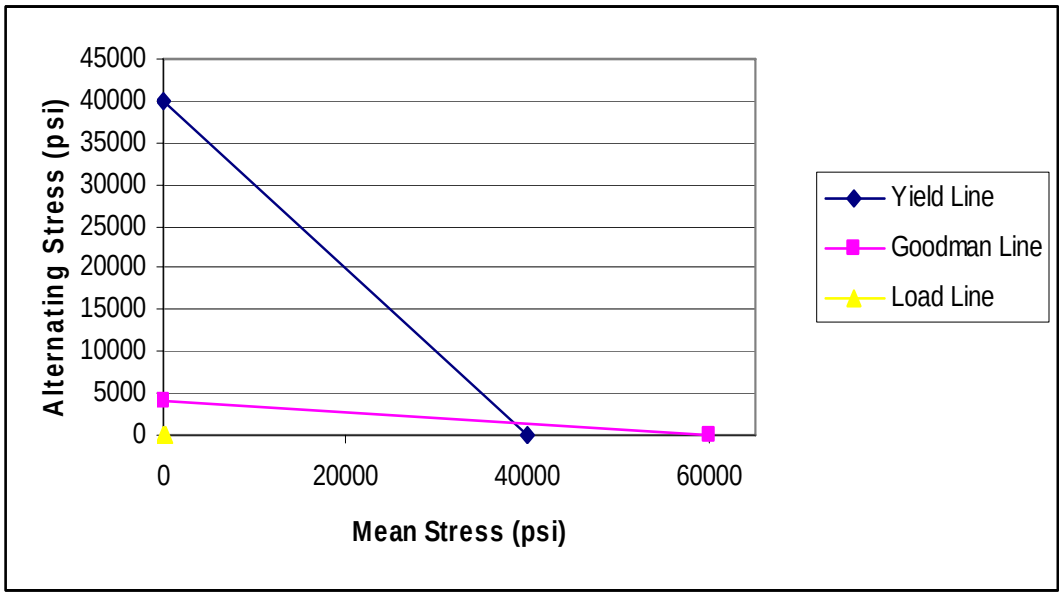

Figure 39 – Arm bolt hole Goodman diagram

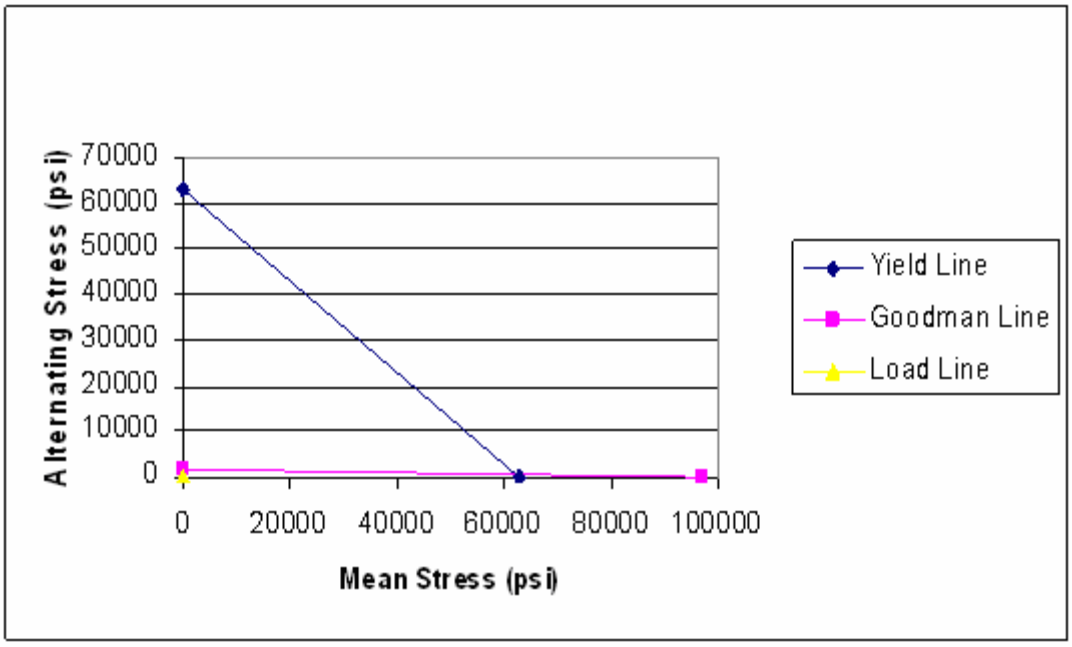

Figure 40 – Shaft Goodman diagram

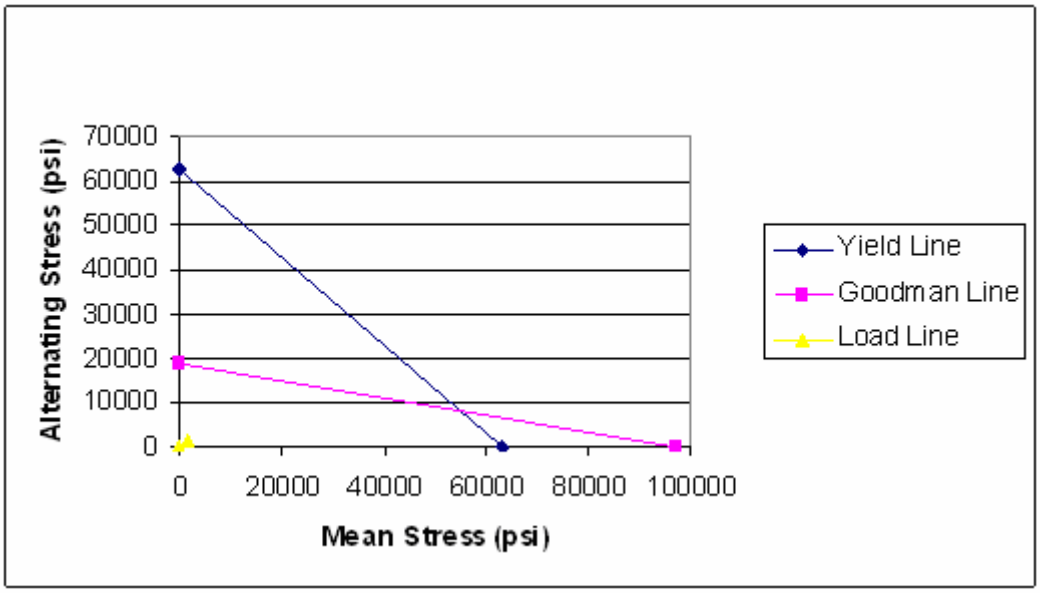

Figure 41 – Key Goodman diagram